

# Neural Responses during Interception of Real and Apparent Circularly Moving Stimuli in Motor Cortex and Area 7a

Hugo Merchant<sup>1,2</sup>, Alexandra Battaglia-Mayer<sup>1,2</sup> and Apostolos P. Georgopoulos<sup>1,2,3,4</sup>

<sup>1</sup>Brain Sciences Center, Department of Veterans Affairs Medical Center, Minneapolis, MN 55417, USA, <sup>2</sup>Department of Neuroscience, University of Minnesota, Minneapolis, MN 55455, USA, <sup>3</sup>Department of Neurology, University of Minnesota, Minneapolis, MN 55455, USA and <sup>4</sup>Department of Psychiatry, University of Minnesota, Minneapolis, MN 55455, USA

**We recorded the neuronal activity in the arm area of the motor cortex and parietal area 7a of two monkeys during interception of stimuli moving in real and apparent motion. The stimulus moved along a circular path with one of five speeds (180–540°/s), and was intercepted at 6 o'clock by exerting a force pulse on a semi-isometric joystick which controlled a cursor on the screen. The real stimuli were shown in adjacent positions every 16 ms, whereas in the apparent motion situation five stimuli were flashed successively at the vertices of a regular pentagon. The results showed, first, that a group of neurons in both areas above responded not only during the interception but also during a NOGO task in which the same stimuli were presented in the absence of a motor response. This finding suggests these areas are involved in both the processing of the stimulus as well as in the preparation and production of the interception movement. In addition, a group of motor cortical cells responded during the interception task but not during a center → out task, in which the monkeys produced similar force pulses towards eight stationary targets. This group of cells may be engaged in sensorimotor transformations more specific to the interception of real and apparent moving stimuli. Finally, a multiple regression analysis revealed that the time-varying neuronal activity in area 7a and motor cortex was related to various aspects of stimulus motion and hand force in both the real and apparent motion conditions, with stimulus-related activity prevailing in area 7a and hand-related activity prevailing in motor cortex. In addition, the neural activity was selectively associated with the stimulus angle during real motion, whereas it was tightly correlated to the time-to-contact in the apparent motion condition, particularly in the motor cortex. Overall, these observations indicate that neurons in motor cortex and area 7a are processing different parameters of the stimulus depending on the kind of stimulus motion, and that this information is used in a predictive fashion in motor cortex to trigger the interception movement.**

**Keywords:** apparent stimuli, area 7A, motor cortex, real stimuli

## Introduction

A very common behavior in animals is to generate movements towards moving objects. For example, intercepting or hitting objects is an important part of the behavioral repertoire of primates, including humans. For a successful interception, subjects need to take into account both the visual information about the moving object and the parameters of the interception movement. At the neurophysiological level, several aspects of interception behavior have been studied separately. For example, a wealth of information has been accumulated regarding the neural mechanisms of visual motion in the

middle temporal area, MT, and the medial superior temporal area, MST (Albright, 1984; Maunsell and Van Essen, 1983a; for a review, see Andersen, 1997), as well as regarding the encoding and decoding of kinetic and kinematic aspects of movement in the motor cortex (for a review see Evarts, 1981; Georgopoulos, 1999). In addition, it has been demonstrated that the visual superior temporal areas are connected to the posterior parietal cortex (PPC; Cavada and Goldman-Rakic, 1989b; Maunsell and Van Essen, 1983b), which in turn is linked to the dorsal and ventral premotor areas (Johnson *et al.*, 1996; Marconi *et al.*, 2001). Thus, due to its connectivity and functional properties, the PPC has been described as an association area involved in sensory integration, spatial attention, coordinate transformation and the formation of early plans for movement execution based on visual information (Colby and Goldberg, 1999; Battaglia-Mayer *et al.*, 2001; Andersen and Buneo, 2002). In fact, several studies have demonstrated the tight functional link between particular regions of PPC and premotor cortex during reaching and grasping stationary objects (Caminiti *et al.*, 1998; Sakata *et al.*, 1998; Rizzolatti and Luppino, 2001). However, even though the parieto-frontal system is an obvious candidate to be engaged in the interception of moving stimuli, little is known about the neural mechanisms in these areas that subserve the sensorimotor integration and predictive processes involved in the interception moving targets.

In initial psychophysical experiments, human subjects were instructed, and monkeys were trained, to intercept stimuli that moved with different accelerations and total travel times (Lee *et al.*, 1997; Port *et al.*, 1997). It was found that the subjects could adopt one of three strategies to initiate an interception movement: one concordant with the threshold distance model, another following the threshold time-to-contact ( $\tau$ ) model, or one that was a combination of the previous two (Port *et al.*, 1997). The first model assumes that the interceptive movement is initiated after the stimulus travel distance reaches a certain threshold value (Collewyn, 1972; van Donkelaar *et al.*, 1992), whereas the second supposes that the movement is initiated when the instantaneous first-order estimate of the time to arrival attains a particular threshold (Lee, 1976). The results of neurophysiological studies using this task showed that the activity of groups of motor cortical neurons was modulated by the parameters of the moving stimulus, the time-to-contact, and/or the kinematics of interception movements (Lee *et al.*, 2001; Port *et al.*, 2001). In the present study we investigated the neural mechanisms of two areas in the parieto-frontal system underlying the interception behavior. Specifically, we determined the functional properties of neurons in motor cortex and area 7a during interception of real or

apparent circularly moving stimuli. Preliminary results have been reported (Merchant *et al.*, 2001a).

## Materials and Methods

### Animals

Two male rhesus monkeys (*Macaca mulatta*, 4 and 7 kg body wt) were used in these experiments. Animal care conformed to the principles outlined in the *Guide for Care and Use of Laboratory Animals* (National Institutes for Health publication no. 85-23, revised 1985). The experimental protocol was approved by the Institutional Review Board.

### Visual Display

Stimuli were back-projected on a tangent screen using a LCD projector (NEC Multisync MT 820/1020). The tangent screen was 69 × 69 cm and was placed 48.5 cm in front of the animal. The moving stimulus was a black circle of 1.44 cm (1.7° of visual angle [DVA]), and traveled on a low contrast circular annulus of 15.2 DVA outside diameter and 1.7 DVA width (Fig. 1). The stimuli could move in real or apparent motion (Fig. 1A) with one of five angular velocities: 180, 300, 420, 480 and 540°/s. In the real motion condition the stimulus was displayed every 16.7 ms, resulting in a smooth stimulus motion, which was indistinguishable from a continuously moving stimulus. In the apparent motion condition five stimuli were flashed successively for 16.7 ms at the vertices of a regular pentagon. The ISI in this condition was 400, 240, 166.6, 150 and 133.4 ms for the speed of 180, 300, 420, 480 and 540°/s, respectively. All the stimuli traveled counter-clockwise (CCW). Finally, the starting points for real moving stimuli were: 216, 198, 144, 126 and 108°, and for apparent moving stimulus were: 72, 36, 288, 288 and 0° for the speeds of 180, 300, 420, 480 and 540°/s, respectively. These starting positions were chosen based on the threshold of minimum processing time to intercept the stimulus in its first revolution, quantified in a previous paper (Merchant *et al.*, 2003a).

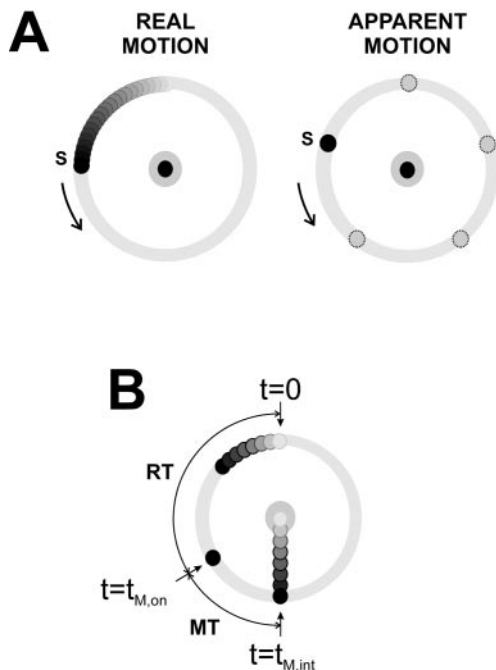


**Figure 1.** Interception task. (A) S represents the smoothly moving stimulus in the real motion condition, and the flashing stimulus at the vertices of a regular pentagon in the apparent motion condition. (B) Behavioral times are defined: RT = reaction time, from  $t = 0$  to  $t = t_{M,on}$  (movement onset), and MT = movement time, from  $t = t_{M,on}$  to  $t = t_{M,int}$  (end of interception).

## Tasks

### Interception Task

In this task the monkeys were seated in a primate chair and operated a semi-isometric joystick (Measurement Systems Inc., Model 467-G824, Norwalk, CT) to intercept moving stimuli. The joystick was a vertical rod placed in front of the monkey at midsagittal level and controlled a net force-feedback cursor which was displayed in the monitor as a circle of 1.7 DVA in diameter (Fig. 1B). The  $x$ - $y$  force exerted by the monkey on the joystick was sampled every 5 ms. The feedback cursor was deflected constantly by 0.85 DVA upward to simulate a bias force of 0.108 N and reflected, at any given moment, the net force, i.e. the vector sum of this simulated force and the force exerted by the animal on the joystick. At the beginning of the trial, the animal had to place the force-feedback cursor within a gray circle of 3.4 DVA in diameter ('center window', located at the center of the screen) by exerting a minimum of 0.108 N of force in the downward direction and keep it there for a variable delay period (1000–3000 ms), after which the stimulus began to move. The monkeys intercepted the moving stimulus by applying a net force pulse on the joystick (minimum 0.89 N) such that the force feedback cursor intercepted the moving stimulus at 6 o'clock (i.e. 270°). This experimental configuration was such that, in the apparent motion condition, the monkeys intercepted a stimulus that crossed the 6 o'clock position in a perceptual rather than in a physical sense. After the interception (when the cursor crossed the gray path), the screen was frozen and the position of the stimulus and the feedback cursor at interception was shown for 200 ms. This provided to the monkeys some feedback about their interception performance. Monkeys received a liquid reward if the angle between the cursor and the stimulus was  $<18^\circ$ . This version of the task was performed by both monkeys without eye position constrains. In addition, monkey 2 was trained in the interception task with eye fixation. In this paradigm, a trial started when the monkey fixated, within 2 DVA window, a yellow point (1 DVA in diameter) located at the center of the center window. Then, the force feedback cursor was presented, and the animal had to place it within the center window. The cursor was to be kept in the center window for a variable delay period (1000–3000 ms), after which the stimulus began to move. The monkey had to intercept the stimulus at 6 o'clock, and after the interception movement was completed the animal continued to fixate for an additional 200 ms. At the end of this period, a reward was delivered if the angle between the cursor and the stimulus was less than  $18^\circ$ . The  $x$ - $y$  eye position was monitored using an oculometer (Dr Bouis, Karlsruhe, Germany). Both the eye and the joystick position were sampled at 200 Hz; the tangential eye velocity was calculated by differentiating eye position. The reaction time (RT) was defined as the period from the beginning of the stimulus movement to the moment at which the force pulse exceeded the mean + 2 SD of the force during the control period, considered the beginning of the movement (Fig. 1B). The movement time (MT) corresponded to the period between the beginning of the movement of the cursor and the time at which the force pulse reached 0.89 N, a force level that corresponded to the feedback cursor crossing the low contrast path (Fig. 1B). Finally, the total experimental time (TET) was:  $TET = RT + MT$ . The different combinations of stimulus velocities and motion conditions were interleaved and presented in a pseudorandom order. A repetition consisted of five trials in the real motion condition and of five trials in the apparent motion condition (with the same five stimulus velocities). Usually five repetitions were collected in each task.

### NOGO Task

The same target speeds, motion conditions and starting points were used. However, in order to cue the animals and distinguish the interception from the NOGO task, a red instead of a gray center window was presented. At the beginning of the trial, the animal had to place the force feedback cursor within the red center window for a variable delay period (1000–3000 ms), after which the stimulus moved for 2000 ms. The monkeys were trained to fixate, within 2 DVA, a yellow dot (1 DVA in diameter) located at the center of the center window, for the duration of stimulus presentation. The animals received a liquid reward if the cursor was maintained inside the center window

throughout the entire trial. Five repetitions of this task were performed in a randomized block design.

#### Center → Out Motor Task

In this task the monkeys produced semi-isometric force pulses on the joystick in 8 radial directions, in response to the presentation of a peripheral stimulus on an imaginary circle of 0.89 N force radius. A force feedback cursor on the screen indicated the current net force exerted on the joystick; a constant upward bias of 0.108 N was applied, corresponding to a deflection of the cursor of 0.85 DVA. A trial began with the appearance of a light spot at the center of the screen which prompted the monkey to exert a downward force of 0.108 N on the joystick to align the force feedback cursor to the center spot within a circular force window of 0.217 N radius. Then, after a variable delay of 1000–3000 ms, a light spot appeared in one of eight locations, separated by 45° and with an eccentricity of 6.8 DVA, which prompted the monkey to apply a force pulse (>0.89 N) on the joystick such that the force feedback cursor would move in the direction of the peripheral stimulus for the monkey to obtain a liquid reward. Five repetitions of this task were performed in a randomized block design.

#### Neural Recordings

Impulse activity of single neurons was recorded extracellularly from area 7a and the proximal arm area of the motor cortex (left hemisphere) (for details, see Merchant *et al.*, 2001b). All isolated neuronal potentials were recorded regardless of their activity during the task, and the recording sites changed from session to session. The presentation of the visual stimuli, behavioral control and data collection were carried out by a personal computer. Online raster displays were generated on a computer monitor.

#### Electromyographic (EMG) Activity

The EMG activity was recorded in separate sessions from the neural recordings using intramuscular, multistranded, Teflon-coated wire electrodes (Schwartz *et al.*, 1988). EMG activity of the following muscles was recorded in the first monkey, contralateral to the recording side: rhomboideus major, trapezius, deltoideus (anterior, middle and posterior), pectoralis major, triceps brachii, biceps brachii, extensor digitorum communis and forearm flexor (unspecified). The same muscles were recorded from in the second monkey, with the addition of supraspinatus, infraspinatus and latissimus dorsi. The EMG signal was amplified, rectified, filtered and sampled at 200 Hz.

#### Data Analysis

##### General

An analysis of covariance (ANCOVA) was performed for each neuron, using the motion condition and stimulus speed as factors and the discharge rate (based on spike counts) during the last 500 ms of the control-holding period as the covariate. The frequency of discharge during the TET was the dependent variable. The spike counts were square-root transformed to stabilize the variance (Cox and Lewis, 1966; Snedecor and Cochran, 1989). The program 2V of the BMDP/Dynamic statistical package (BMDP Statistical Software Inc., Los Angeles, CA) was used to execute the ANCOVA. In addition, for those neurons that did not show statistically significant effects on the ANCOVA, we performed a one-way analysis of variance (ANOVA) between the discharge rate during the control period and TET, to identify the cells that showed general changes in their activity during interception. The level of statistical significance to reject the null hypothesis for all statistical analyses was set at  $\alpha = 0.05$ . The results of the ANCOVA and the ANOVA were consistent between monkeys and were combined. Cells were included in the analysis if they were recorded during the interception, the NOGO and the center → out tasks for at least four repetitions. In addition, the neurons required to have a mean firing rate >0.6 impulses/s. Of a total of 910 cells recorded in area 7a, 766 fulfilled the criteria above and analyzed further. In motor cortex, 1112 cells were recorded and 776 fulfilled the criteria and analyzed further.

#### Spike Density Functions

The spike trains for each trial in the task were converted to 1 ms spike density functions using the fixed kernel method with a Gaussian pulse of 20 ms (Richmond and Optican, 1987).

#### Activation Periods

An activation period was defined as the interval during the TET where the mean spike density function for a particular stimulus speed and motion condition exceeded the mean + 3 SD of the control spike density function during the 500 ms before stimulus onset.

#### Multiple Linear Regression with an Autoregressive Error Component

We investigated the relations between the time-varying cell activity during the interception task and the stimulus position, the time-to-contact, and the vertical hand force and hand force velocity (see below). However, since during the interception task the monkeys could move their eyes freely, it was necessary to account for the neural signals related to eye position, before performing an analysis of the stimulus and hand movement parameters. For that purpose, we carried out a multiple linear regression analysis between the time-varying single cell activity and eye position. An autoregressive component was added to the regression model to take in to account the correlation between residuals that occurs in time series regression. The model was the following:

$$f_t = b_0 + b_1 x_t + b_2 y_t + u_t \quad (1)$$

$$u_t = \rho u_{t-1} + \varepsilon_t$$

where  $f_t$  is the SDF at time  $t$ ,  $b_0$  is a constant,  $b_1$  is the regression coefficient of the  $x$  coordinate of the eye position at time  $t$ ,  $b_2$  is the regression coefficient of the  $y$  coordinate of the eye position,  $\rho$  is the first-order autoregressive coefficient, and  $\varepsilon_t$  is a normally distributed, uncorrelated random error with variance  $\sigma^2$  and mean = 0. This regression model was performed using the data of real and apparent motion stimuli. The statistical significance of the regression model was determined using an  $F$ -test ( $P < 0.01$ ). In order to account for eye position related signals, we used the residuals of the eye position regression as the dependent variable in the next multiple regression model (see equation 2). However, these residuals were used as dependent variables in equation (2) only if the neurons showed significant eye position effects. Otherwise, the original SDF was used as dependent variable.

Once the eye position regression was performed, we computed a multiple linear regression in order to evaluate the relations between the cell activity and the stimulus position (angle  $\theta$ ), the time-to-contact ( $\tau$ ), and the vertical hand force and its rate of change. An autoregressive component was added again to the regression model which was defined as:

$$f_t = b_0 + b_1 \cos \theta_{t+\Delta 1} + b_2 \sin \theta_{t+\Delta 1} + b_3 \tau_{t+\Delta 2} + b_4 y'_{t+\Delta 3} + b_5 \dot{y}'_{t+\Delta 3} + u_t \quad (2)$$

$$u_t = \rho u_{t-1} + \varepsilon_t$$

where  $f_t$  is the SDF or the residual (with respect to eye position) at time  $t$ ,  $b_0$  is a constant, and  $b_1$ – $b_5$  are the regression coefficients,  $\rho$  is the first-order autoregressive coefficient, and  $\varepsilon_t$  is an uncorrelated, normally distributed random error with variance  $\sigma^2$  and mean = 0. This regression was performed separately for the real and apparent motion conditions and for different lags ( $\Delta 1$ ,  $\Delta 2$  and  $\Delta 3$ ) between the SDF and the stimulus and movement parameters. The time lag  $\Delta 1$  was the stimulus angle lag and varied from -160 to +160 ms,  $\Delta 2$  was the time-to-contact lag and also varied from -160 to +160 ms, and finally,  $\Delta 3$  was the hand force lag and varied from 0 to +160 ms. These three time lags were utilized so that the time shifts of the stimulus, the time-to-contact and the hand force could be assessed independently, and were shifted in 40 ms intervals. Therefore a total of 405 regression models were performed for each motion condition in every cell. The regression with the largest  $R^2$  in the real and apparent motion conditions was used as the final model for each neuron.

A detailed collinearity analysis was performed on the independent variables. High values of tolerance values (>0.4) were observed for all

variables. (The tolerance is calculated as  $1 - R^2$  for an independent variable when it is predicted by the other independent variables already included in the analysis.) Therefore, we concluded that the variables used in our model did not covary substantially. In both regression models (equations 1 and 2) we used the Cochrane-Orcutt method, which consisted of an iterative process to optimize  $\rho$ , as stated in SPSS 7.0 Statistical Algorithms (procedure AREG; SPSS Inc., Chicago, IL).

#### Analysis of Frequencies of Occurrence of Significant Parameter in the Regression

The above multiple linear regression analysis identified the variables that showed a significant effect on the neural activity. However, this analysis did not identify which parameters were associated or showed concurrent significant effects in a single cell. For this purpose, we constructed six  $2 \times 2$  tables for all possible pairs of variables (e.g. stimulus angle and hand force) containing the frequency of significant and non significant cases. Chi-square statistics (two-tailed) were used to determine the level of statistical significance of association between pairs of variables. In addition, we calculated the  $\phi$  coefficient that can range from -1 to +1, and that not only expresses the strength of an association between variables, but also the direction of the association. These analyses were carried out for both areas in the real and apparent motion conditions.

## Results

### Behavioral Performance

The primary measure of performance was the angular error in direction, defined as the signed angle,  $\theta$ , between the stimulus and the feedback cursor when the cursor crossed the middle of the low contrast path (Fig. 2A). As can be seen in this figure, there was a slight difference between the real and apparent motion conditions but in both of them  $\theta$  was near zero for all stimulus speeds, with a small increase with increasing speed. This directional error differed significantly among stimulus speeds in both monkeys and in both types of stimulus motion (ANOVA,  $P < 0.0001$ ). This indicates that both monkeys could intercept the real and apparent moving stimuli with a high level of accuracy, although there was a tendency to make

systematic late interceptions as the speed increased. The performance of the two monkeys was very similar and consistent, and thus the data were combined.

The SD of the angle  $\theta$ , named variable error in direction, increased as a linear function of the stimulus speed in the real motion condition, and was systematically higher for the apparent motion situation (Fig. 2B). In fact, both the stimulus speed and the motion condition showed significant effects in the ANOVA ( $P < 0.0001$ ). The stimulus position at the beginning of the interception movement (SAI) decreased asymptotically as a function of the stimulus speed in both motion conditions (Fig. 2C). The ANOVA showed significant effects of both motion conditions and target speed factors ( $P < 0.0001$ ). Finally, the movement time decreased slightly as a function of the stimulus speed and was larger in the real than in the apparent motion condition (Fig. 2D), with significant effects on both variables (ANOVA,  $P < 0.0001$ ).

In summary, the performance of both monkeys in the interception task was very accurate, with a small tendency to make late interceptions as a function of the speed in both motion conditions, and an increase in the variability of the angle error in the apparent motion situation. Regarding the strategy followed to initiate the interception movement, it was difficult to assign a particular model to the real and apparent motion data, since the movement time and the SAI were not constant. For example, according to the threshold distance model, the interception movement should start at a constant distance from the interception zone, but in this case the SAI decreased as a function of the stimulus speed. On the other hand, the threshold time-to-contact ( $\tau$ ) model states that the interception movement should start at a constant  $\tau$ , but the movement time decreased as stimulus speed increased.

### Neural Responses to Real and Apparent Motion Stimuli during the Interception Task

A total of 776 neurons in the motor cortex and 766 neurons in area 7a fulfilled the criteria for number of trials and strength of responses in all tasks, and were analyzed further (see Methods). In the motor cortex, 502/776 (64.7%) cells showed statistically significant effects in the interception tasks, including 306 (39.4%) cells with significant effects of motion condition and/or stimulus speed in the ANCOVA, and 196 (25.3%) cells with statistically significant differences between the control and TET. In area 7a, 450/766 (58.7%) cells showed statistically significant effects in the interception tasks, including 321/766 (41.9%) cells with significant effects of motion condition and/or stimulus speed in the ANCOVA, and 129/766 (16.8%) cells with significant changes in activity between the control and the visual stimulation period (RT) was the following: 188/776 (24.2%) in the motor cortex and 125/766 (16.3%) in area 7a.

The number of neurons with statistically significant effects of motion condition, stimulus speed and/or, motion condition  $\times$  stimulus speed interaction is listed in Table 1. An important group of neurons showed selective responses during real or apparent motion. In fact, the motion condition main effect was the most important factor driving the cell activity in both areas, followed by the motion condition  $\times$  stimulus speed interaction. These results suggest that different neural systems were active

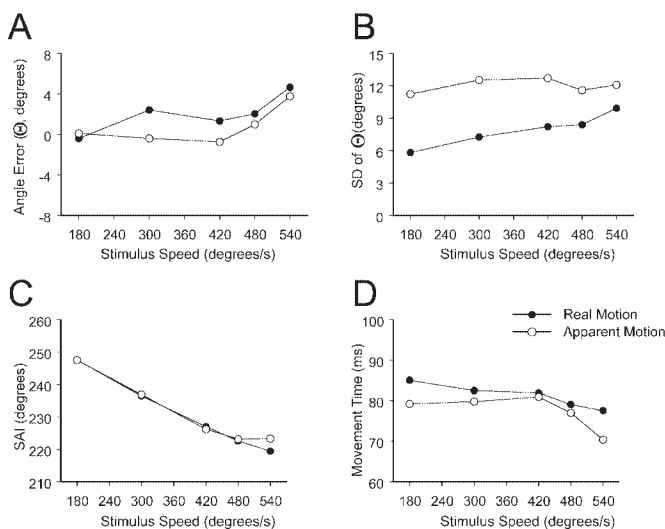


**Figure 2.** Behavioral performance of the two monkeys in the interception task. (A) Angle error ( $\Theta$ ); (B) SD of  $\Theta$ ; (C) position of the stimulus at the beginning of the interception movement (SAI); and (D) movement time are plotted as a function of the stimulus speed. Filled circles correspond to the real motion and open circles to the apparent motion condition.

**Table 1**

Numbers and percentages (in parentheses) of neurons with the noted effects during the interception task in the ANCOVA

Effect	Motor cortex	Area 7a
Motion condition only	151 (30.1)	188 (41.8)
Stimulus speed only	44 (8.8)	19 (4.2)
Motion × speed interaction	111 (22.1)	114 (25.3)
Task epoch	196 (39)	129 (28.7)
Total	502 (100)	450 (100)

during real and apparent motion interceptions in the motor cortex and area 7a. We investigated this further, as follows.

### Time-varying Multiple Linear Regression

One of the primary objectives of the present study was to characterize the relations between the neural activity over time and different aspects of the stimulus and the hand response in both motion conditions. However, since the interception task was performed by both monkeys without eye position constrain, it was necessary to take into account a possible effect of eye position on the neural activity when determining the relations above. For this purpose, we first assessed the effect of eye position by using a time-varying multiple regression analysis and then removing it, if statistically significant, by taking the residual SDF and using it as the dependent variable in the main regression analysis. Thus, the relations between SDF and stimulus and hand parameters were determined independently of any eye position effects. These parameters included the cosine and sine of the stimulus angle, the time-to-contact ( $\tau$ ) of the stimulus with respect to the interception zone ( $270^\circ$ ), and the hand vertical force and rate of force change (see Methods). The regression was carried out using different time lags between the neural activity and the stimulus angle,  $\tau$  and the hand force in an independent fashion, ranging from  $-160$  to  $160$  ms in  $40$  ms steps (see Methods). The model with the best coefficient of multiple determination ( $R^2$ ) for each cell during the real and apparent motion conditions were considered further if they showed a statistically significant effect ( $P < 0.001$ ,  $F$ -test). For these models the residuals were examined for the presence of systematic trends (Draper and Smith, 1981). No such trends were observed, which indicated that the obtained models were valid. An example of the residuals plotted against the predicted values is shown in the right panels of Figure 3A,B. The percentage of neurons with a significant regression model, and with at least one significant factor ( $P < 0.01$ ,  $t$ -test on the regression coefficient) was  $515/776 = 66.4\%$  in the motor cortex and  $356/766 = 46.5\%$  in area 7a. Most of these cells showed a significant regression model in the real or the apparent motion condition, and only 171 (171, 515, 33.2%) of the neurons in motor cortex and 39 (39/356, 10.9%) in area 7a showed significant regressions in both motion conditions. The  $R^2$  of the statistically significant regressions varied substantially among cells, ranging from 0.055 to 0.76 in motor cortex, and 0.055 to 0.62 in area 7a; this spread can also be appreciated in the cumulative distribution plots of the  $R^2$  (Fig. 4). These distributions differed significantly between the two areas ( $P < 0.007$ , Kolmogorov-Smirnov test, two-tailed); the median  $R^2$  was higher in the motor cortex ( $R^2 = 0.138$ ) than in area 7a ( $R^2 =$

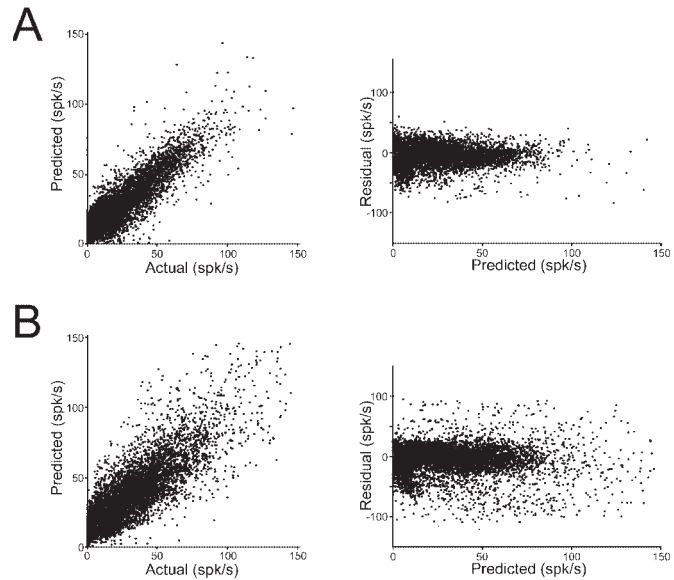


**Figure 3.** Scatter plots of predicted values against the actual SDF values (right panel), and predicted values against the residuals (left panel). (A) Motor cortical neurons ( $n = 128$ ) with a  $R^2 > 0.35$ . (B) Area 7a neurons ( $n = 92$ ) with  $R^2 > 0.2$ .

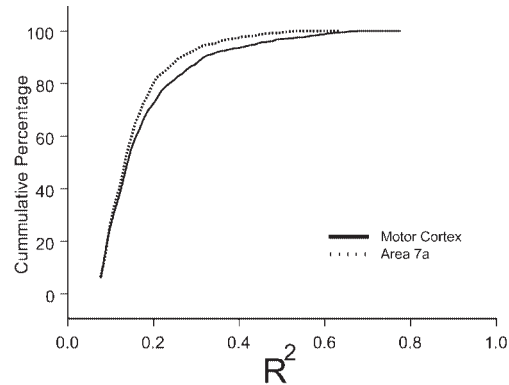


**Figure 4.** Cumulative distribution of the proportion of variance explained ( $R^2$ ) in motor cortex and area 7a.

0.125). These results document an engagement of varying strength of cells in both areas in the interception process. Next, we examine more specific aspects of this engagement.

Three different measures were used to characterize the relation between the neural activity and the stimulus and hand movement parameters (Ashe and Georgopoulos, 1994). These measures were calculated in those regressions that showed a significant  $R^2$  ( $F$ -test,  $P < 0.01$ ). The first measure was the standardized regression coefficients, which were rank-ordered to determine the explanatory power of each parameter in relation to the other parameters. The results of this analysis showed clear differences between the real and apparent motion conditions (Fig. 5). In the real motion condition, the hand force was the most important parameter for the motor cortex, whereas for area 7a was stimulus position. In contrast, in the apparent motion condition,  $\tau$  was the most important parameter in the motor cortex followed by the hand force (Fig. 5A), whereas in area 7a the time-to-contact and the stimulus position were the

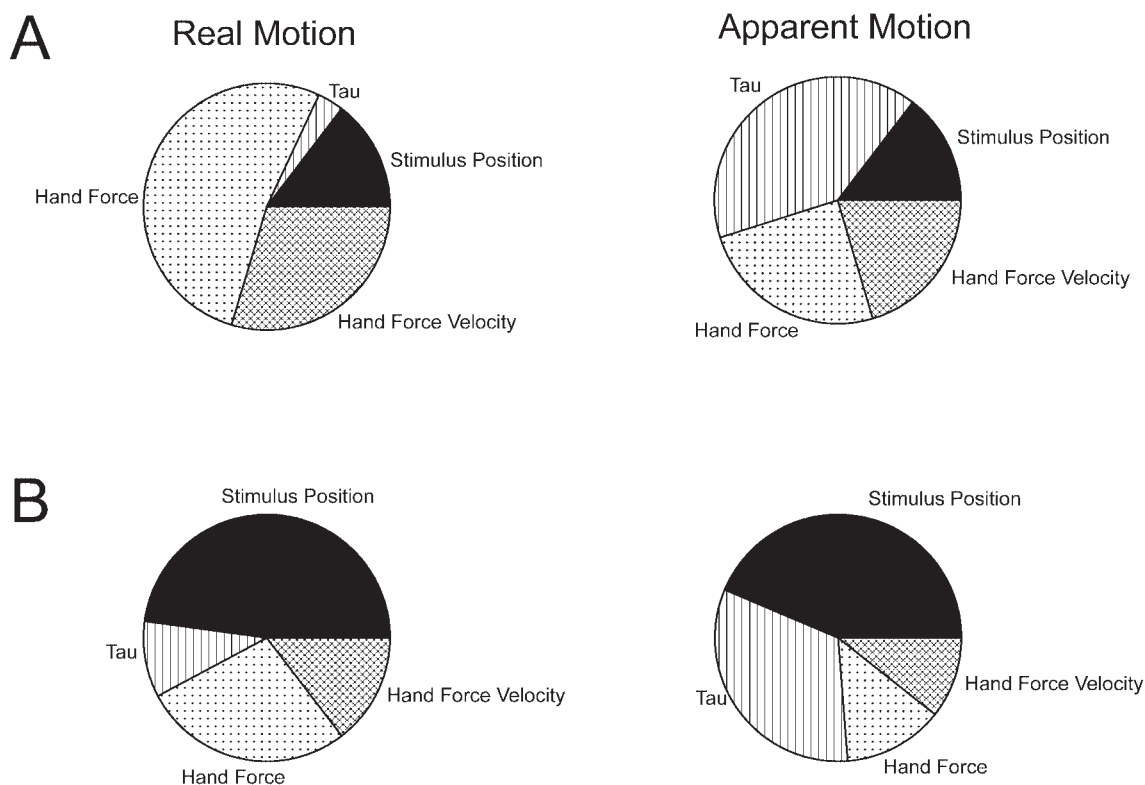


**Figure 5.** Percentages of neurons in the real and apparent motion conditions, during the interception task without eye fixation, for which the noted parameter was ranked first in the standardized coefficients analysis (see text for more details). (A) Motor cortex. (B) Area 7a.

most important parameters (Fig. 5B). Interestingly, very similar results were obtained when the same analysis was carried out in the interception task with eye fixation in monkey 2 (Fig. 6). The second measure was the percentage of times for which each parameter was statistically significant ( $P < 0.01$ ,  $t$ -test), without taking into account the importance of that parameter in relation to the other parameters (Table 2). The results of this analysis were similar to the first measure. Finally, the third measure was the number of significant parameters in every multiple linear regression; this measure indicated whether the neural activity was related to one or more parameters. Figure 7 shows that at least one or two of the parameters tested contributed significantly to the time-varying neuronal activity in both areas. However, there was a tendency to present more significant parameters in the motor cortex than in area 7a (Fig. 7).

A substantial proportion of cells in area 7a and motor cortex showed more than one significant parameter in their regression model. Hence, we were interested to determine whether particular combinations of variables were associated in the same cell with a frequency that was above chance. Specifically, we sought to establish whether the processing of sensory variables was associated to the encoding of motor variables, and whether there were differences in these relations between the real and apparent motion conditions in both areas. For this purpose, the results of the regression analysis were analyzed further by categorizing the result of the significant testing for each parameter in a dichotomous fashion (presence or absence of a significant effect). This produced counts of binary outcomes for stimulus angle,  $\tau$ , hand force and force velocity that were used to construct  $2 \times 2$  contingency tables, between

the six possible combinations of variable pairs. We tested the significance of associations between these variables using  $\chi^2$  statistics and the  $\phi$  coefficient (see Methods). The results of this analysis are shown in Figure 8, where it is clear that the association between the sensory and motor parameters was very different in the two areas and both motion conditions. In the motor cortex during the real motion condition the hand force was significantly associated with the hand force velocity and the stimulus angle, whereas during apparent motion, the hand force was significantly coupled with  $\tau$  and the hand force velocity. In addition, in area 7a for the real motion condition the stimulus angle was significantly associated with the hand force velocity, and  $\tau$  was significantly coupled with the hand force velocity. Finally, in the apparent motion condition area 7a neurons showed significant associations between the stimulus angle and the hand force and force velocity. It should be noted that the sign of all these associations was negative, as revealed by the  $\phi$  coefficient (Fig. 8), which indicates that significant effects of different variables tended to occur separately, i.e. in different cells.

A different question concerns the time shifts of the stimulus angle, time-to-contact and hand force for which the highest  $R^2$  was obtained for each cell. Since the independent variables were shifted with respect to the neural activity, a negative shift indicated that the variable was leading the neural activity (sensory response), whereas a positive shift indicated that the neural activity was leading the variable (predictive response). In the motor cortex, the neural time shift distributions were skewed towards the predictive side for the motor variables, with a median for the vertical hand force (Fig. 9C) and the

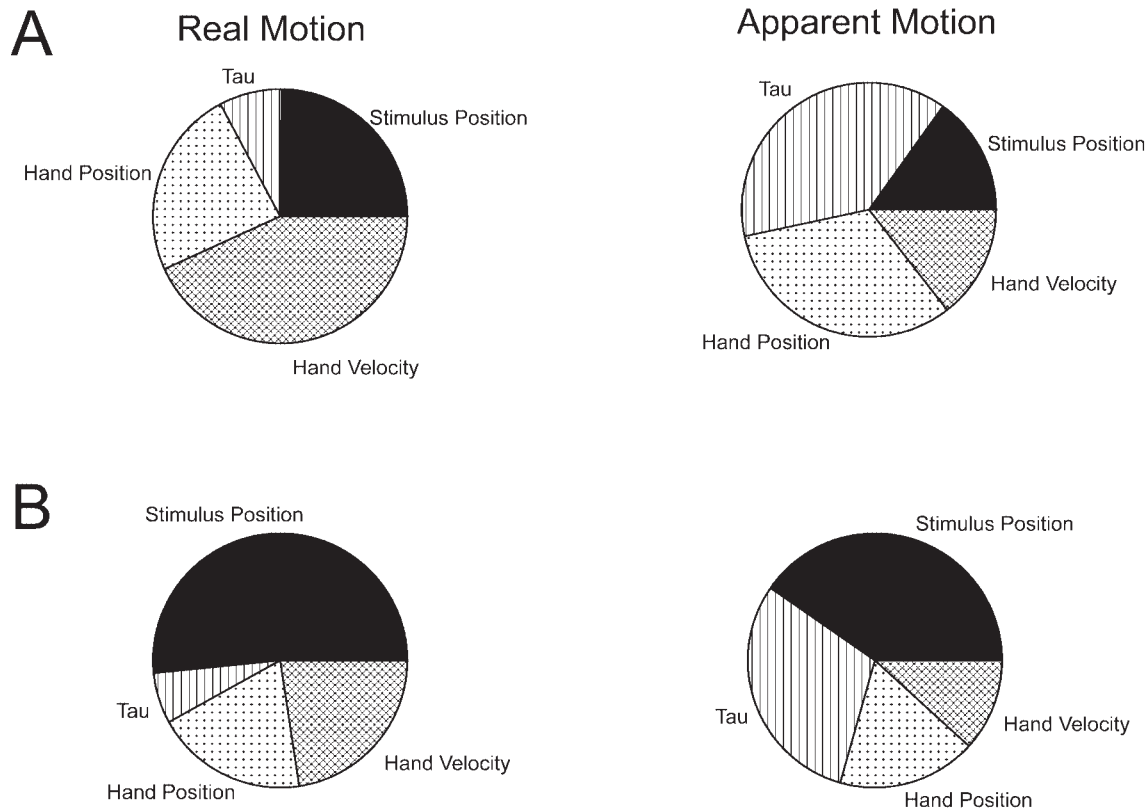


**Figure 6.** Percentages of neurons in the real and apparent motion conditions, during the interception task with eye fixation, for which the noted parameter was ranked first in the standardized coefficients analysis (see text for more details). (A) Motor cortex. (B) Area 7a.

**Table 2**

Numbers and percentages (in parentheses) of neurons for which the noted variable showed a significant effect in the multiple linear regression

Variable	Real motion		Apparent motion	
	Motor cortex	Area 7a	Motor cortex	Area 7a
Stimulus position	102/459 (22.2)	84/209 (40.2)	106/868 (12.2)	204/499 (40.9)
Tau ( $\tau$ )	38 (8.3)	29 (13.9)	270 (31.1)	140 (28.1)
Hand force	175 (38.1)	55 (26.3)	258 (29.7)	90 (18)
Hand force velocity	144 (31.4)	41 (19.6)	234 (27)	65 (13)

vertical hand force velocity (Fig. 9D) of 40 ms. In addition, the distribution of time shifts for the stimulus angle and  $\tau$  were bimodal, with the largest peaks at  $-160$  and  $+160$  ms and with a median of zero in both variables (Fig. 9A,B). No significant differences were found between the distributions in the real and apparent motion conditions for stimulus angle, hand force and hand force velocity (Kolmogorov–Smirnov test,  $P > 0.05$ ), although in the case of the time-to-contact the distributions in the real and apparent motion conditions were significantly different (Kolmogorov–Smirnov test,  $P = 0.02$ ). Therefore, the encoding of the hand parameters in the time varying activity of the motor cortex preceded the change of variables, indicating that the motor cortical neural activity predicted the values of these parameters. In contrast, in area 7a the neural time shift distributions of the stimulus position (Fig. 10A) and  $\tau$  (Fig. 10B) were skewed towards negative values (median  $-80$  ms for both variables), indicating that area 7a neurons were

responding to the change in these stimulus parameters. In addition, the time shift distributions of the neural activity in this area showed a median of 0 ms for vertical hand force (Fig. 10C), and 40 ms for vertical hand force velocity (Fig. 10D). Finally, no significant differences were found between these distributions in the real and apparent motion conditions in area 7a (Kolmogorov–Smirnov test,  $P > 0.05$ ).

#### Task Comparisons

The results of the multiple linear regression analysis showed that the neural activity in motor cortex and areas 7a varied over time according to different stimulus and hand force parameters in the interception task. The hand force position and hand force velocity contributed significantly to the variation in neural activity, particularly in the motor cortex. Furthermore, the stimulus position was the most important parameter during real motion, whereas during apparent motion was the time-to-

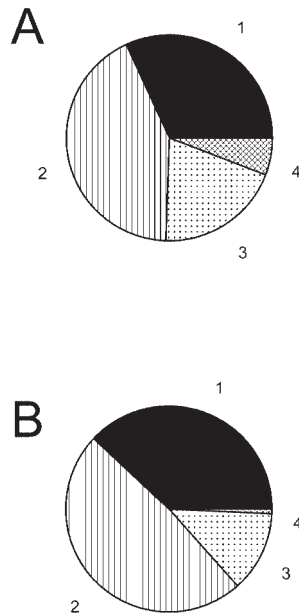


**Figure 7.** Percentages of cells that showed significant effects to the noted numbers of parameters in motor cortex (A) and area 7a (B).

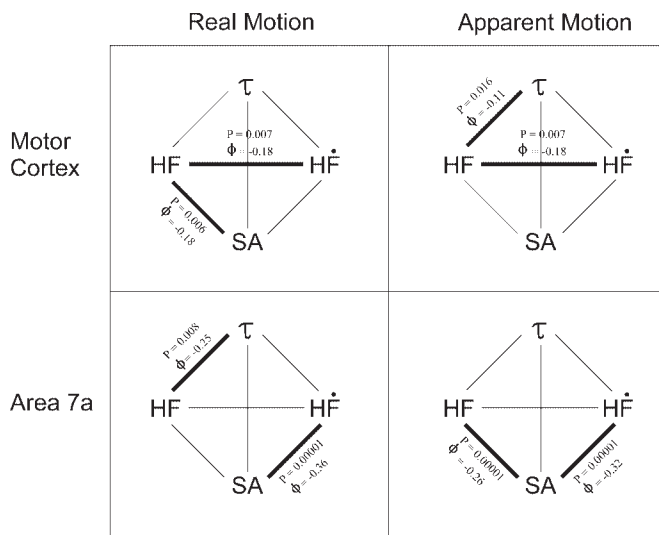


**Figure 8.** Association of sensory and motor parameters by cells in the motor cortex and area 7a during the real and apparent motion conditions in the interception task. Thick lines connecting pairs of variables indicate significant associations in the  $2 \times 2$  tables using a  $\chi^2$  test. The numbers adjacent to the lines represent the P value of the  $\chi^2$  test and the  $\phi$  coefficient. SA = stimulus angle;  $\tau$  = time-to-contact; HF = vertical hand force (the overdot represents its velocity).

contact ( $\tau$ ). These results suggest that different sensory-motor aspects of the interception task are encoded dynamically in the neural activity of both areas, with a clear dichotomy in sensory processing between real and apparent motion conditions, particularly in the motor cortex. In the sections that follow, we compared the neural responses of cells during different tasks in an effort to determine whether these dynamic neural signals were context-dependent. Specifically, we compared the activity of neurons during the following tasks: interception, NOGO, center  $\rightarrow$  out, and interception task with eye fixation.

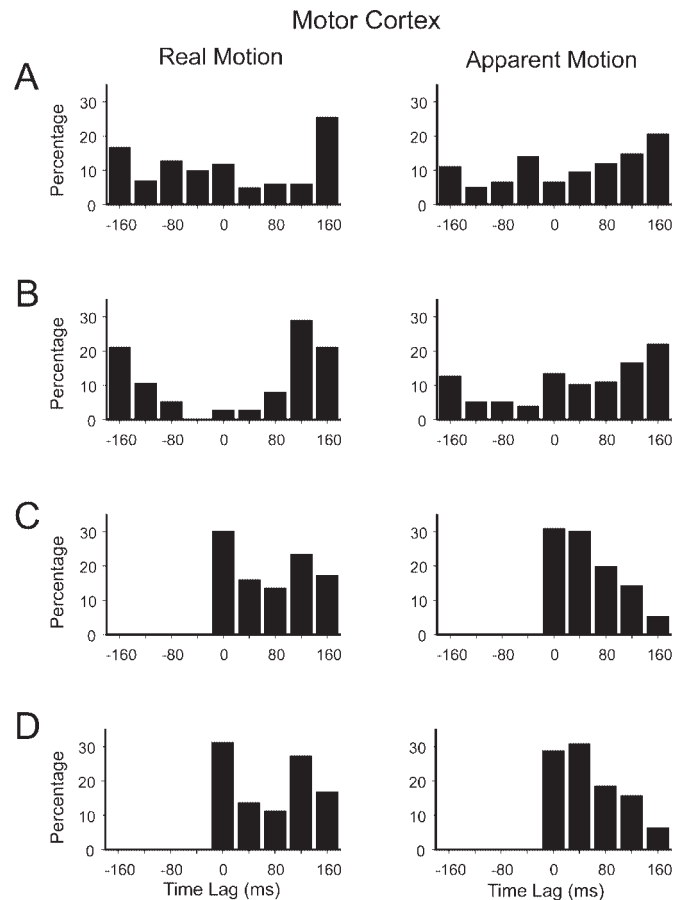


**Figure 9.** Distribution of the time lags at which the largest  $R^2$  was obtained in the real and apparent motion conditions in the motor cortex for the different parameters used in the multiple regression model. (A) Stimulus angle. (B) Time-to-contact. (C) Vertical force. (D) Vertical force velocity.

These direct comparisons, allowed for the dissection of neural responses in the following categories: (i) visual responses to moving stimuli; (ii) motor activity involved in the production of the force pulse; (iii) neuronal activity potentially associated with the predictive process involved in the interception of the stimulus; and (iv) effects of the saccades and eye position on neural activity.

### Comparison of the Neural Responses in the Interception and NOGO Tasks

We performed an ANCOVA on the neuronal activity during the NOGO task. The results are shown in Table 3. Comparing these results with the ANCOVA for the interception task data described above (Table 1), it was evident that more motor cortical neurons were modulated during the interception ( $n = 502$ , 64.7%) than during the NOGO task ( $n = 347$ , 44.7%; see Table 3). This is not surprising, since in the NOGO task the monkeys did not execute a motor response. Furthermore, the number of neurons in area 7a with significant effects in the ANCOVA was very similar in the interception ( $n = 450$ , 58.7%) and NOGO tasks ( $n = 436$ , 56.9%; see Table 3).

Next we carried out a paired  $t$ -test analysis between the discharge rate of neurons during the control period and during the first 750 ms of the reaction time in both tasks separately.

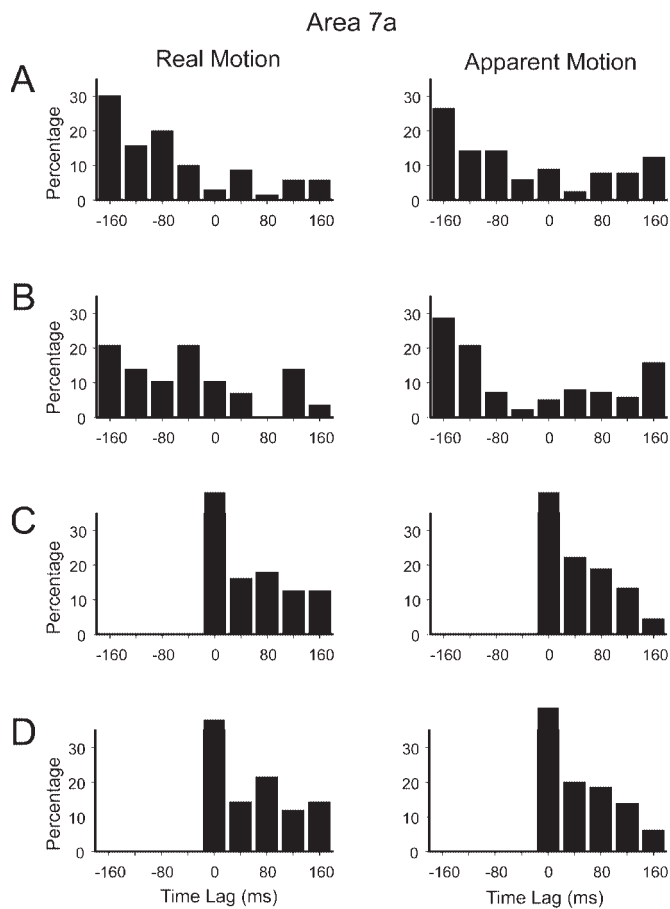


**Figure 10.** Distribution of the time lag at which the largest  $R^2$  was obtained in the real and apparent motion conditions in area 7a for the different parameters used in the multiple regression model. (A) Stimulus angle. (B) Time-to-contact. (C) Vertical force. (D) Vertical force velocity.

The results revealed that in the motor cortex 273/776 (35.2%) cells showed a significant relation only to the interception task, 61/776 (7.8%) cells showed a significant relation only to the NOGO task, and 97/776 (12.5%) cells showed significant relations to both tasks. The same analysis in area 7a revealed the following: 170/766 (22.2%) cells showed a significant relation only to the interception task, 96/766 (12.5%) cells showed a significant relation only to the NOGO task, and 150/766 (19.6%) cells showed significant relations to both tasks. Thus, in summary, more neurons were active during the interception task than during the NOGO task, predominantly in the motor cortex. Nevertheless, it is possible that the neural responses in the latter task may be involved in visual motion processing.

The analyses above assessed the overall difference in the cell activity between the interception and NOGO tasks. However, in order to characterize the dynamic patterns of activation during the two tasks, we performed a more detailed analysis for each motion condition and stimulus speed as follows. First, we determined the ‘activation periods’ during which the mean SDF was above the mean + 3 SD of the control SDF (1000 ms before stimulus onset; see Methods). Next, the discharge rate throughout each activation period was compared between the interception and NOGO tasks, using a one-way ANOVA. This analysis allowed the identification of three different cell types: (i) cells with significantly larger responses during the inter-

**Table 3**

Numbers and percentages (in parentheses) of neurons in motor cortex and area 7a with the noted effects during the NOGO task in the ANCOVA

Effect	Motor cortex	Area 7a
Motion condition only	88 (25.4)	126 (28.9)
Stimulus speed only	23 (6.6)	20 (4.6)
Motion × speed interaction	47 (13.5)	50 (11.5)
Task epoch	189 (54.5)	240 (55)
Total	347 (100)	436 (100)

ception than the NOGO task; (ii) cells with responses that did not differ in the two tasks; and (iii) cells with significantly larger responses during the NOGO than the interception task. Figure 11 shows the rasters and SDF for motor cortical cells corresponding to types 1 (Fig. 11A) and 2 (Fig. 11B). Similarly, Figure 12 shows examples of neurons in area 7a pertaining to the cell types 1 and 2. The numbers of cases (5 stimulus speeds × 2 motion conditions = 10 cases) in the motor cortex and area 7a corresponding to different types of cells are illustrated in Figure 13. In both areas, neurons with significantly greater responses during the interception task (type 1) were more common than neurons with greater responses in the NOGO task (type 3), or with similar responses in both tasks (type 2), particularly in the motor cortex. These results indicate that a larger population of neurons is activated during the interception of moving stimuli than during the passive presentation of moving stimuli in the NOGO task.

We investigated then how the temporal profile of activation varied across cell types and areas. Figure 14 illustrates the population SDF for the activation periods of cells with significantly larger responses during the interception task in the motor cortex (filled, gray line) and in area 7a (open, black line). The population SDF for the interception task is shown in Figure 14A aligned to the stimulus onset, and in Figure 14C aligned to the onset of the interception movement. In Figure 14B,D, the NOGO population SDF is illustrated aligned to the stimulus onset and to the beginning of the interception movement, respectively. It is evident that area 7a neurons not only showed an earlier response onset than the motor cortex neurons, but their responses were also best aligned to the stimulus onset (Fig. 16A). In contrast, the activation periods in the motor cortex were best aligned to the movement onset (Fig. 14B,C).

The number of neurons and cases with significantly larger responses during the NOGO than the interception task (type 3) was very small in both areas (Fig. 13). Finally, neurons in area 7a with similar responses during the interception and NOGO task (type 2) had activation periods that were best aligned to the stimulus onset, and occurred earlier than those observed for the same type of responses in the motor cortex (Figs 15 and 16A). In the motor cortex, the activation periods were best aligned to the interception movement. It is important to mention that most type 2 cells in the motor cortex (79.2% of the cases) and area 7a (66.8% of the cases) responded to real but not to apparent moving stimuli in the NOGO task.

The overall onset latencies of the two groups of cells (types 1 and 2) are shown in Figure 16. When the PSDFs were aligned to the stimulus onset, the onset latencies of area 7a cell types 1

## Motor Cortex

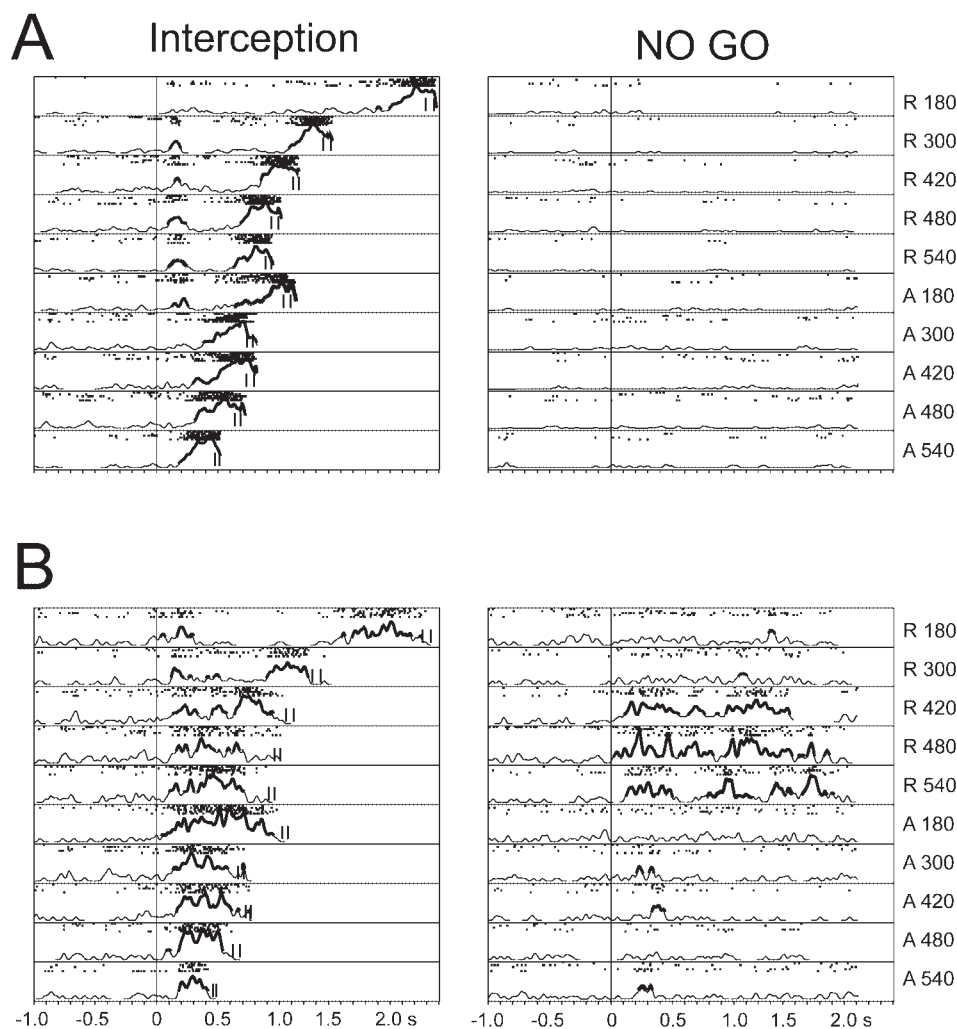


**Figure 11.** Rasters of spike trains (top) and mean spike density functions (bottom) for each motion condition and stimulus speed of two motor cortical cells during the interception and NOGO tasks. (A) Neuron that responded during the interception, but not in the NOGO task. (B) Neuron that was activated during the interception task in both motion conditions that also responded in the real motion condition during the NOGO task. The neural activity of five trials was aligned to the onset of the stimulus movement (0 s). The black bold portions indicate that the SDF was above the mean + 3 SD of the control period. The large vertical lines at the bottom of each raster represent the beginning and end of the interception movement. R, real motion; A, apparent motion. Stimulus speed is in degrees/s.

and 2 appeared consecutively, followed by the motor cortical cell types 1 and 2 (Fig. 16A). Cell type 1 in the motor cortex showed long onset latencies and a large variance, because the activity was not well aligned to the onset of the stimulus. On the contrary, this type of motor cortical cells showed an onset latency closer to the beginning of the movement, followed by motor cortical cell type 2 and cell type 1 in area 7a (Fig. 16B).

In conclusion, most of the motor cortical neurons showed an increase in discharge rate prior the onset of the interception movement, and did not respond in the NOGO task. These neurons may be engaged in the execution of the interception movement. However, an important group of motor cortical cells also responded during the NOGO task, with patterns of activation aligned to the onset of the stimulus motion. In addition, neurons in area 7a showed earlier responses to the onset on the moving stimulus during the interception and NOGO tasks, or during the interception task alone. This parietal activation was probably associated with visual processing of motion

and the sensorimotor transformation that was taking place to trigger the interception movement. Interestingly, in both areas most of the neurons that responded during the interception and NOGO tasks (type 2) showed a selective activation for real moving stimuli.

### **Comparison of the Neural Responses in the Interception and Center → Out Tasks**

Once the neurons with visual properties during the interception task were characterized, we determined the nature and temporal profile of the motor responses during the interception and center → out tasks in the motor cortex. First, we identified those neurons which showed a significant increase in discharge rate (from the control period) during the last 350 ms of the RT and during the MT in the interception task. Then, we identified those neurons that showed in the center → out task either a significant increase in discharge rate during the same epochs, or a significant effect of movement direction.

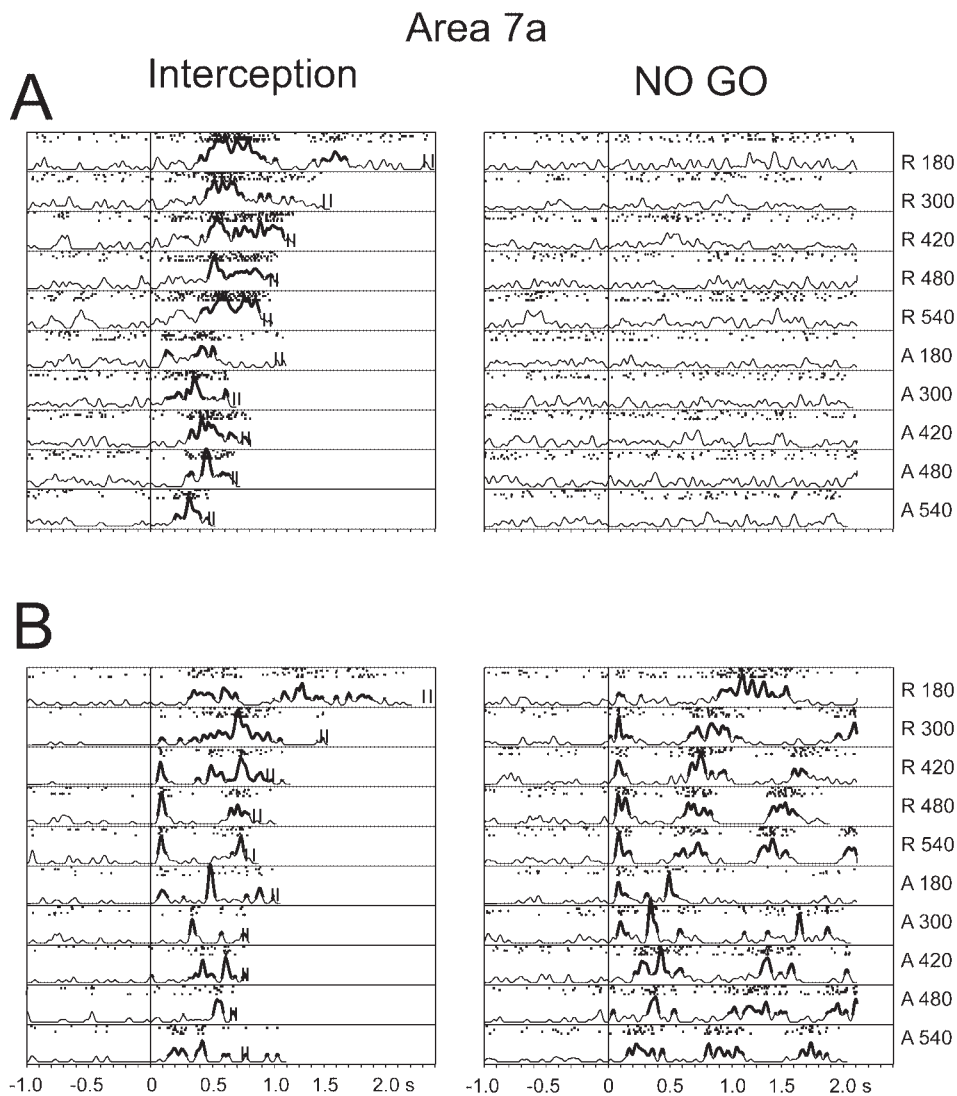


**Figure 12.** Rasters and mean spike density functions of two cells in area 7a during the interception and NOGO tasks. (A) Neuron that responded exclusively during the interception task. (B) Neuron that was similarly activated during the interception task and NOGO task. The same conventions as in Figure 11.

A group of neurons (216/776, 27.8%) showed significant relations in both tasks (Fig. 17C). In addition, 54/776 (7%, Fig. 17A) cells showed a significant relation only to the interception task, whereas 249/776 (32.1%, Fig. 17B) cells showed a significant relation only to the center → out task. The remaining 257/776 (33.1%) of the motor cortical cells did not show significant effects in either task.

In both tasks the animal applied a force pulse in the joystick to move the cursor in the appropriate direction to get the stimulus. However, in the interception task this force pulse was always exerted downward (270°), whereas in the center → out it was applied in eight directions. Therefore it is not surprising that the preferred direction distribution of most of the cells with a significant modulation only during the center → out task was skewed, avoiding the 270° direction used in the interception movement (Fig. 17B; mean angle 112°; Rayleigh test,  $P = 0.003$ ; see Mardia, 1972). In contrast, the preferred direction distribution of the cells that showed significant relations to both tasks was evenly distributed (Fig. 17C; Rayleigh test,  $P = 0.308$ ).

Thus in general, neurons that responded during the last part of the reaction time and during the movement time in the interception task, also responded during the center → out task. These neurons, then, were probably involved in the force pulse generation in both tasks. Nevertheless, it is interesting that a group of motor cortical cells responded exclusively during the interception task, suggesting their involvement in the sensorimotor transformations taking place in this task. These responses were probably engaged in the link of visual motion signal to the predictive mechanism that controls the initiation of the interception movement.

#### ***Neural Responses in the Interception with and without Free Eye Movements***

The neural activity during the interception of moving stimuli with or without eye fixation requirements was compared in monkey 2 using two different measures. First, we compared the proportions of neurons that showed significant effects in motion condition and/or stimulus speed (ANCOVA,  $P < 0.05$ ), or a significant increase in discharge rate between the control

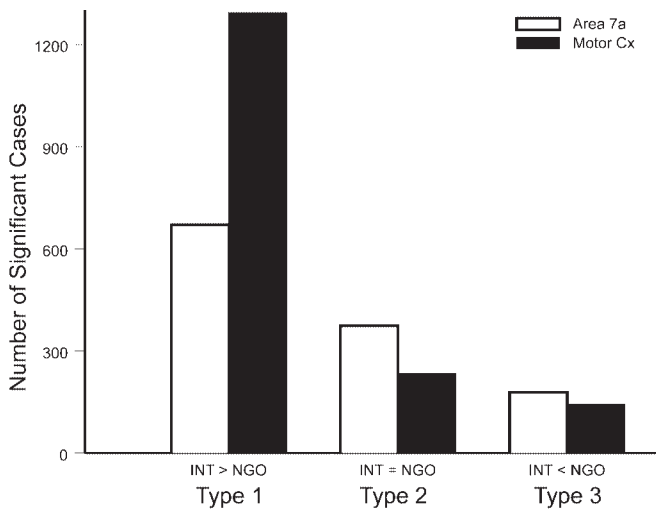


**Figure 13.** Number of significant cases (each cell has 10 cases, 5 stimulus speed  $\times$  2 motion conditions) in the motor cortex and area 7a for different effects in the activation periods comparison between the interception and NOGO tasks. Filled black bars correspond to motor cortex and open bars to area 7a data.

period and the TET (ANOVA,  $P < 0.05$ ) in these two tasks. Table 4 shows the results of these analyses, where it is evident that the proportion of significant cells between the interception task with or without eye fixation was very similar in both areas. In fact, the number of significant cells did not differ significantly between the two tasks in area 7a ( $\chi^2 = 4.92$ ,  $df = 3$ ,  $P = 0.178$ ), or motor cortex ( $\chi^2 = 2.88$ ,  $df = 3$ ,  $P = 0.41$ ).

The second comparison measure was a paired t-test between the discharge rates during the TET in the two tasks. We found that 313/399 (78.5%) and 272/357 (76.2%) neurons in motor cortex and area 7a, respectively, did not show significant differences. Nevertheless, in motor cortex 33/399 (8.3%) neurons showed a larger discharge rate during interceptions without eye fixation, and 53/399 (13.3%) during interceptions with eye fixation. In area 7a, 45/357 (12.6%) neurons showed a larger discharge rate during the interception task without eye fixation requirements, as did 40/357 (11.2%) during the interception task with eye fixation. These results indicate that although most of the neurons in both areas showed similar discharge rates when the monkey was performing the interception with or without the eyes fixated, there was a neural population that might be related to eye fixation, and another

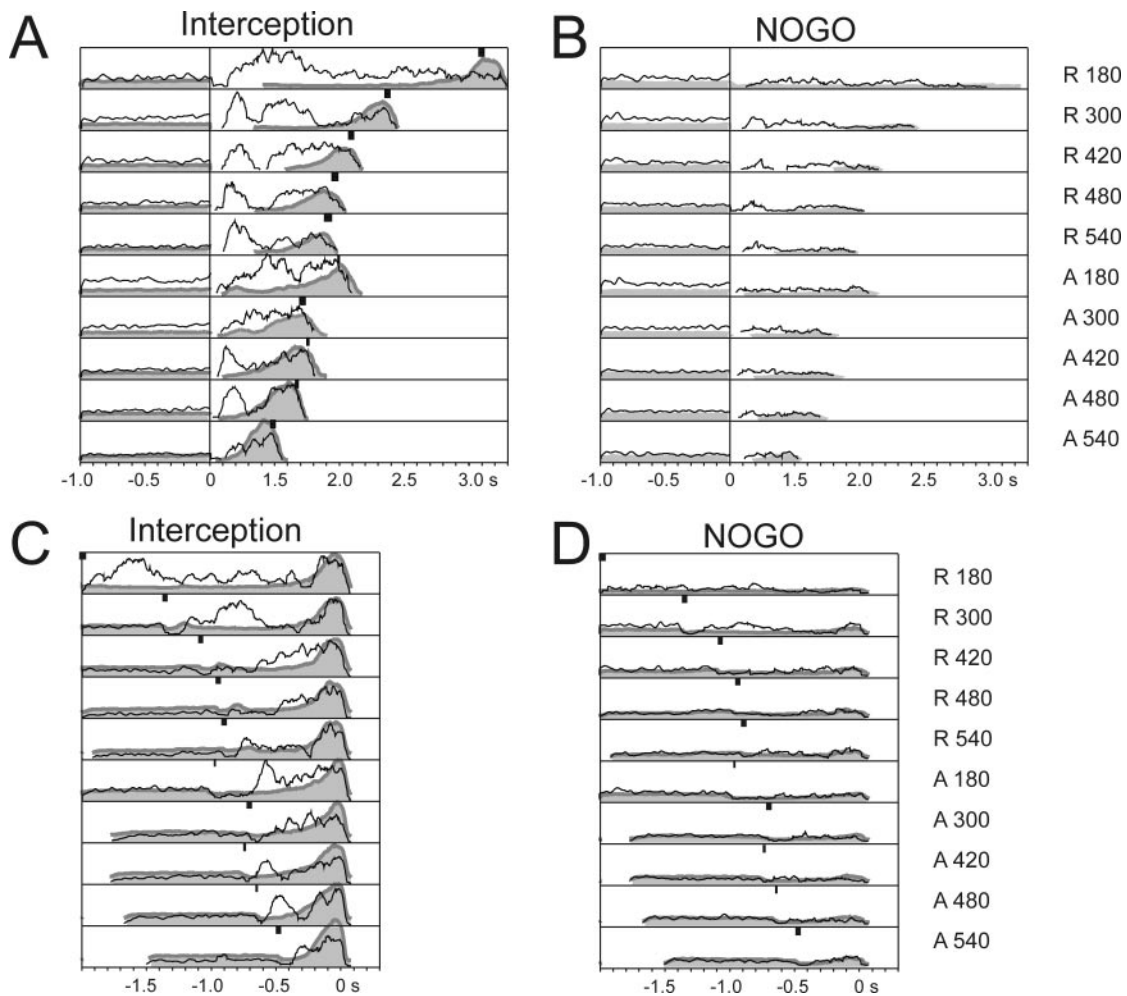


**Figure 14.** Population spike density functions of neurons in the motor cortex (filled gray) and area 7a (open) with significantly larger responses during the interception than the NOGO task (type 1). (A) and (B) correspond to the interception and NOGO tasks, respectively, aligned to the onset of the stimulus movement (0 s). (C) Interception and (D) NOGO tasks aligned to the movement onset during the interception task (0 s). Black rectangles at the top of each condition represent in (A) the mean  $\pm$  SD of the movement onset, and in (C) and (D) the mean  $\pm$  SD of the stimulus onset during the recording of these neurons.

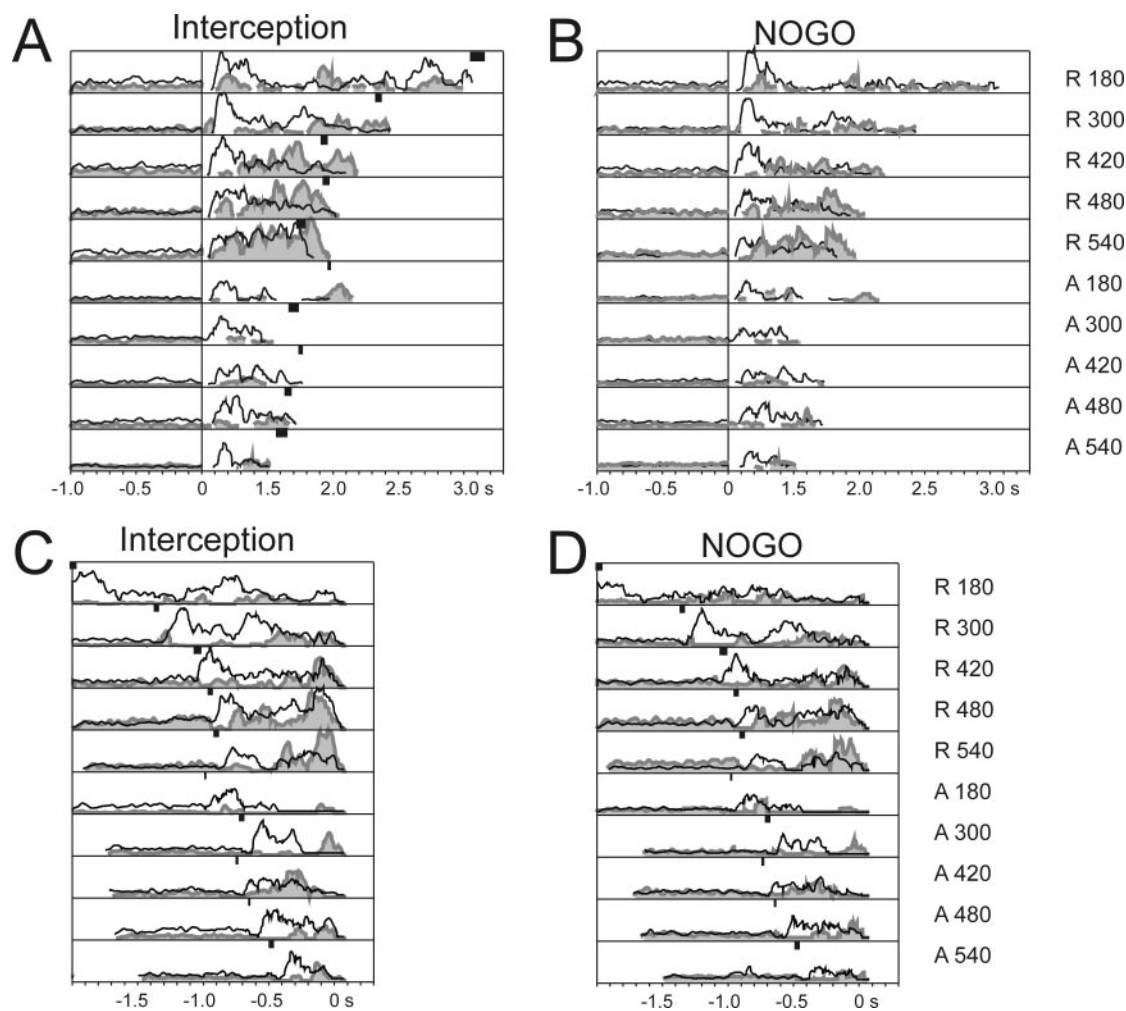


**Figure 15.** Population spike density functions of neurons in the motor cortex (filled gray) and area 7a (open) cells with similar responses in the two tasks during activation periods (type 3). (A) Interception and (B) NOGO tasks aligned to the onset of the stimulus movement (0 s). (C) interception and (D) NOGO tasks aligned to the movement onset during the interception task (0 s). Look to the higher responses in the real motion condition during the NOGO task. Same conventions of Figure 14.

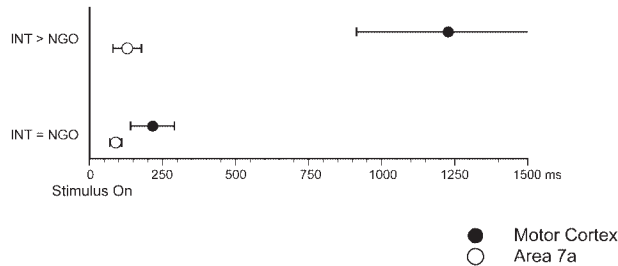
population associated with the eye movements performed during the interception task. In fact, post-saccadic and eye position signals have been previously reported in area 7a (Barash *et al.*, 1991). Nevertheless, the difference in cell properties during the interception with or without eye fixation is too small to explain the large effects of motion condition, stimulus speed, stimulus angle, time-to-contact, hand vertical force and force velocity described in the previous sections. In fact, as we mentioned above, the multiple regression analysis showed that similar proportions of neurons showed significant effects on the stimulus and hand-arm parameters during the interception with (Fig. 6) and without eye fixation (Fig. 5). Finally, it should be noted that this experiment was not designed to test the effects of eye movements *per se* but the possible effects of eye movements on neuronal discharge in the context of this study were accounted for by either controlling the eye position (by eye fixation) or by removing their possible influence using regression analysis.

#### EMG Activity

A time-varying multiple linear regression was performed using the mean EMG activity as the dependent variable, and the

cosine and sine of the stimulus angle, the variable  $\tau$ , the hand vertical force and force velocity as independent variables. This regression was computed for 13 shoulder, upper and forearm muscles (see Methods). Of these muscles the following showed a significant  $R^2$  ( $F$ -test,  $P < 0.01$ ) in the regression: rhomboideus major ( $R^2 = 0.59$ ), pectoralis major ( $R^2 = 0.4$ ), biceps brachii ( $R^2 = 0.66$ ), extensor digitorum communis ( $R^2 = 0.69$ ), supraspinatus ( $R^2 = 0.34$ ), infraspinatus ( $R^2 = 0.3$ ) and latissimus dorsi ( $R^2 = 0.38$ ). In most of these muscles, the standardized coefficient that was ranked 1 was the hand force. These included in the real motion situation, the rhomboideus major, pectoralis major, biceps brachii, extensor digitorum communis and latissimus dorsi. In the apparent motion condition, the muscles where the hand force standardized coefficient was ranked 1 included: the rhomboideus major, pectoralis major and extensor digitorum communis. In addition, in the apparent motion condition the rate of change of hand force was the coefficient ranked 1 in the biceps brachii and the latissimus dorsi. Finally, the standardized coefficient of  $\tau$  was ranked 1 only in the supraspinatus and infraspinatus, and the standardized coefficient of stimulus angle was never ranked 1 in any muscle. The median of the time shift at which the highest  $R^2$

A



B

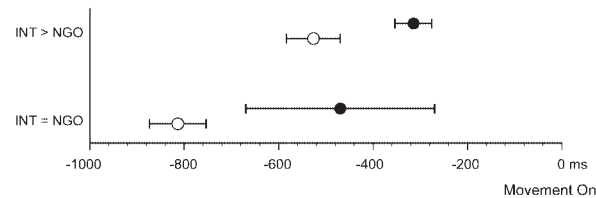


**Figure 16.** Onset latencies (Mean  $\pm$  SEM) of the population spike density functions of type 1 neurons (INT > NOGO; see Fig. 14) and type 3 neurons (INT = NOGO; see Fig. 15). (A) onset latencies when the neural activity was aligned to the stimulus onset. (B) onset latencies when the activity was aligned to the interception movement onset. Filled circles correspond to motor cortex and open circles to area 7a.

were observed was 20 ms for the real motion and 0 ms for the apparent motion condition.

Overall, these results indicated that the EMG activity of most of the shoulder, upper and forearm muscles during the interception task showed a clear time-varying relationship with the hand force and hand force velocity. Therefore, the EMG activity did not account for the tight relation between the neural activity and the stimulus position and/or  $\tau$  observed in a large group of cells in the motor cortex and area 7a (see above).

## Discussion

In this study we examined the descriptive and quantitative relations between the neural activity in motor cortex and area 7a, and various stimulus and movement parameters of interception. Two main complementary results were obtained. First, a group of neurons in each area responded in the interception and NOGO tasks, indicating that the stimulus processing and the preparation and production of the interception movement depends on a distributed system engaging frontal and parietal areas. Secondly, a multiple regression analysis revealed that the sensory variables were better represented in the activity of area 7a neurons during interception task, whereas the motor parameters were better accounted for in the activity motor cortical cells. Nevertheless, the neural activity in area 7a showed a clear modulation by motor variables, and the motor cortical activity showed also a representation of sensory parameters. In fact, this analysis also revealed that during the real motion situation the stimulus angle was the most important stimulus parameter encoded in both areas, whereas during the apparent motion condition the time-to-contact became the parameter with the larger explanatory power in the motor cortex. These results suggest that different neural mechanisms are engaged in the perception and sensorimotor transformations associated with the interception of these two types of moving stimuli. These issues are discussed below.

## Different Neural Mechanisms Engaged in the Interception of Real or Apparent Motion Stimuli

The different analyses performed in the present study suggested that partially overlapping neural populations were involved in the processing of interception of real or apparent motion stimuli. First, the ANCOVA showed that most of the neurons in motor cortex and area 7a were activated selectively in the real or the apparent motion conditions, in both the interception and NOGO tasks. Secondly, the multiple linear regression analysis indicated that in the real motion condition, the stimulus direction was the most important stimulus factor to explain the variation in cell activity in area 7a, and was the second most important parameter in motor cortex, preceded by the hand force. Conversely, in the apparent motion condition the time-to-contact,  $\tau$ , was the most important explanatory parameter in motor cortex, and the second most important variable in area 7a. Thus these findings suggest that not only different populations of neurons are involved in the real or apparent motion interceptions, but also that the stimulus parameters encoded by these ensembles were different in the two motion conditions.

The prevalence of stimulus position signals during the real motion situation in the multiple regression analysis suggests that neural populations in motor cortex and area 7a were engaged in processing the stimulus position over time, and that this information was probably used to trigger the interception movement in the real motion condition. This hypothesis is supported by the finding that neurons in motor cortex are modulated by the stimulus position during the real but not during the apparent motion conditions in the NOGO task (Merchant *et al.*, 2003b).

On the other hand, the time-to-contact,  $\tau$ , was the most important explanatory parameter in apparent motion interceptions in motor cortex, and was the second most important in area 7a, preceded by the stimulus angle. This is the first time that a neural correlate of the first-order estimate of the time to arrival is reported in primates. Neurophysiological studies performed in the pigeon and the locust, however, have reported looming-sensitive neurons that signal the time-to-contact using  $\tau$  (Hatsopoulos *et al.*, 1995; Rind and Simmons, 1999).

We assumed that in the apparent motion condition the animals intercepted a stimulus that was the perceptual 'reconstruction' of motion based on a sequence of stationary stimuli (Port *et al.*, 1996). In separate psychophysical experiments performed in nine human subjects, we observed that the detection threshold for apparent motion was  $314^\circ/\text{s}$  (ISI 223.3 ms; H. Merchant *et al.*, unpublished observations). Taking into consideration the similarities in visual processing between human subjects and monkeys, it was possible that at speeds above  $314^\circ/\text{s}$  the monkeys were using the perceptual integration of motion to intercept the apparent moving stimuli. However, we can not rule out the possibility that in this condition the monkeys used the timing between dots to solve the interception task. In fact, we found a population of neurons in area 7a that signaled the onset of the flashing dots during the NOGO task (Merchant *et al.*, 2003b). Therefore, it is possible that this type of neural signal could be the primary source of information for the integration of the time-to-contact. Consequently, a suitable hypothesis is that during the interception of apparent moving stimuli the critical variable was time rather than the stimulus location information.

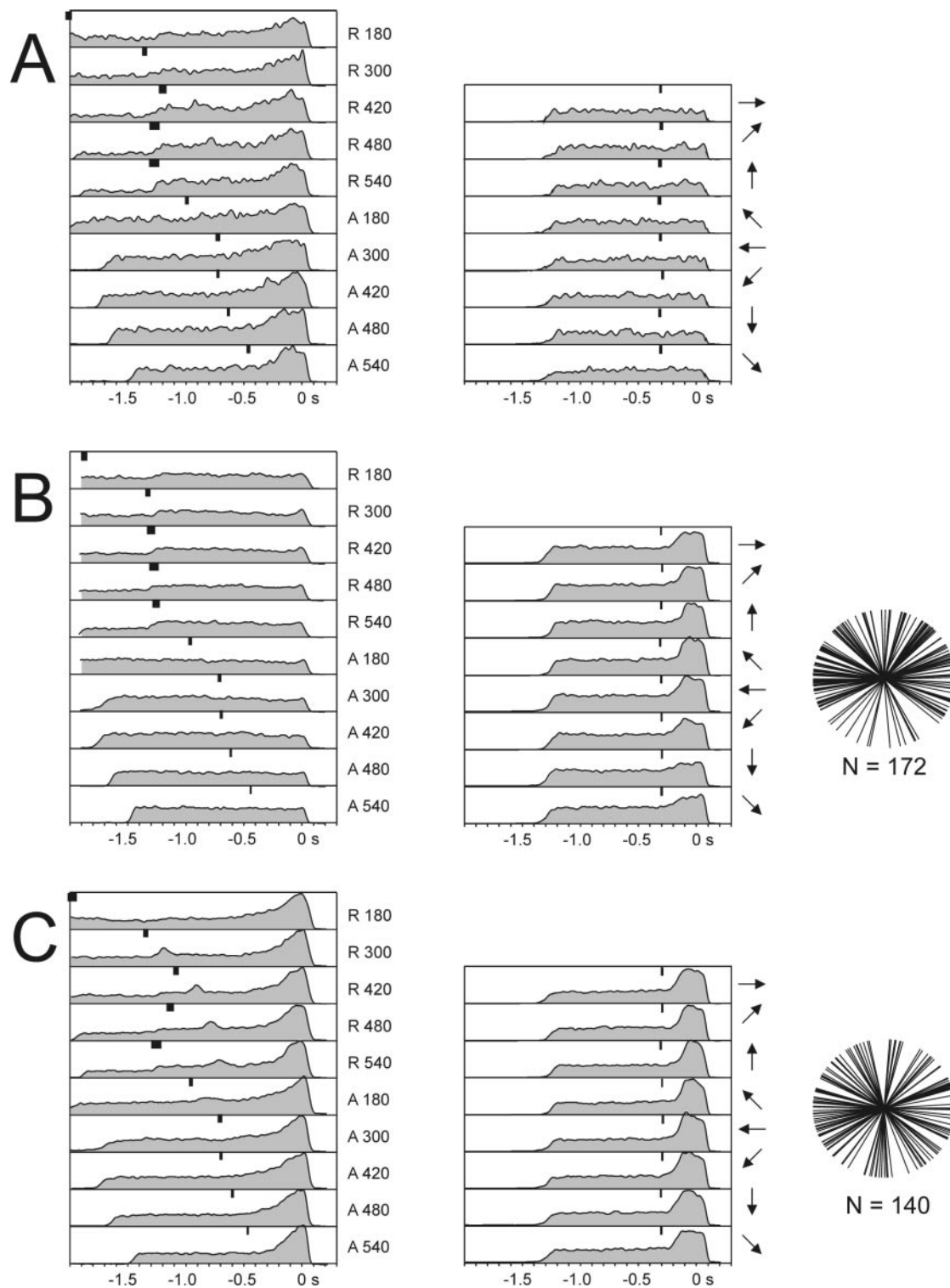


**Figure 17.** Population spike density functions of neurons in the motor cortex during the interception and center → out tasks. (A) Neurons with larger responses during the interception than the center → out task. (B) Neurons with larger responses during the center → out than interception task. (C) Neurons with similar responses in both tasks. Right panel interception task; middle panel center → out task (the arrows point in the direction of the stimulus); left panel preferred directions on the corresponding neurons in the center → out task. The neural activity was aligned to the interception movement onset (0 s). Black rectangles at the top of each condition represent the mean  $\pm$  SD of the stimulus onset during the recording of these neurons.

Most of the neurons that responded during both the interception and NOGO tasks (type 2 neurons) were activated during the real but not the apparent motion condition. In the NOGO task, the stimulus position information was available.

However, the time-to-contact was not a meaningful parameter, since there was no interception. Therefore, this suggests that (i) the neurons that encoded time information did not respond in the two tasks because  $\tau$  was not a relevant variable in the

**Table 4**

Numbers and percentages (in parentheses) of cells with the noted effects during the interception task with or without eye fixation in monkey 2

Effect	Motor cortex		Area 7a	
	Without fixation	With fixation	Without fixation	With fixation
Motion condition	109 (38)	97 (35)	100 (44.3)	90 (38.8)
Stimulus speed	44 (15.3)	52 (18.8)	34 (15)	38 (16.4)
Motion × speed	31 (10.8)	27 (9.7)	42 (18.6)	36 (15.5)
Task epoch	103 (35.9)	101 (36.5)	50 (22.1)	68 (29.3)
Total	287 (100)	277 (100)	226 (100)	232 (100)

NOGO task; and (ii) the type 2 cells were probably associated to the stimulus position.

It is worth mentioning that in area 7a the stimulus position was the most important parameter in the multiple regression analysis during apparent motion, followed by  $\tau$ . These two parameters were processed by different neural ensembles in this area, as revealed by the contingency table analyses. Thus, even if the two stimulus signals were present in area 7a during apparent motion, only the time-to contact signal reached the motor cortex in this situation.

Based on all this evidence, it is possible that the neural mechanisms that controlled the initiation of the interception movement differed in real and apparent motion. We suggest that the neural representation of stimulus position over time was the signal used to initiate the movement during the interception of real moving stimuli. This hypothesis implies that the interception movement could be started when the stimulus position signal reached a specific value, a mechanism that will follow the distance threshold model (van Donkelaar *et al.*, 1992). In contrast, the interception movement in the apparent motion situation was possibly triggered when the neural representation of  $\tau$  reached a particular value. This neural mechanism, then, will follow the threshold  $\tau$  model (Lee, 1976; Port *et al.*, 1997). Nevertheless, it is important to mention that interception behavior of the monkeys did not follow threshold distance or threshold model in the real or apparent motion conditions (Merchant *et al.*, 2003a). Therefore the interception performance of the animals did not validate or reject the hypothesis stated.

#### **Cell Activity Associated to the Interception Movement**

A very interesting finding of this study was the identification of neurons in the motor cortex which responded during the interception task but did not respond during the center → out task. This group of motor cortical cells may encode some features of the sensorimotor transformations taking place during the interception of real and apparent moving stimuli, including the link of visual motion signal to the predictive mechanism that controls the initiation of the interception movement. Nevertheless, the majority of cells responded during both tasks or just during the center → out tasks. In addition, the multiple regression analysis indicated that the hand force was the most important explanatory parameter in the motor cortex in the real motion, and the second most important parameter in the apparent motion condition. These results, then, are concordant with several studies that have demonstrated that the magnitude (Thach, 1978; Evarts, 1981) and predominantly the direction of force are represented in the activity of motor

cortical cells (Georgopoulos *et al.*, 1992; Taira *et al.*, 1996; for review, see Ashe, 1997). Furthermore, the time shift of cell activity for obtaining the highest  $R^2$  was 40 ms, which is consistent with the average shift values obtained in other studies in 2D movement tasks (Humphrey *et al.*, 1970; Schwartz, 1993; Ashe and Georgopoulos, 1994). Finally, the hand force was also an important explanatory parameter in area 7a in the real motion condition, supporting the idea that area 7a neurons produced an early command signal for triggering the interception movement (Mountcastle *et al.*, 1975; see below).

#### **Distributed Neural System Engaged during the Interception Task**

Despite the fact that the neurons in motor cortex responded to visual motion stimulation and to different parameters of the stimulus motion, most of the motor cortical cell activity was driven by the interception movement. In addition, the temporal profile of activation in the motor cortex was linked to the onset of the force pulse (Figs 5, 13 and 14). In contrast the neural activity in area 7a was mostly engaged to the sensory aspects of the interception task, and the neural responses in this area were tightly associated to the onset of the stimulus movement. This suggests that the sensory motor transformations engaged in the interception task include a parieto-frontal distributed system that shows functional gradients. These functional gradients may be defined in large part by the connectivity of its elements (Mountcastle, 1978; Johnson *et al.*, 1996; Battaglia-Mayer *et al.*, 2001).

From the sensory viewpoint, area 7a is reciprocally connected with multiple visual areas including MST, the parieto-occipital area (PO), V2, the fundus superior temporal (FST) and the superior temporal polysensory area (STP) (Cavada and Goldman-Rakic, 1989a). In addition, several studies have indicated that neurons in area 7a respond to complex moving visual stimuli (Motter and Mountcastle, 1981), including rotatory stimuli (Sakata *et al.*, 1986, 1994) and optic flow (Siegel and Read, 1997; Merchant *et al.*, 2001b, 2003b). Indeed, due its connectivity and physiology, area 7a has been considered at the top level of the visual motion dorsal stream (Andersen *et al.*, 1990; Felleman and Van Essen, 1991; Merchant *et al.*, 2003c). Therefore, in the present study it was not surprising to find circular motion signals in area 7a. However, this area is also engaged in the integration of visual information to plan a movement, including the coordinate transformations taking place during visually guided behaviors, and the early planning of reaching movements. Neurons activated during reaching have been reported in this area (Mountcastle *et al.*, 1975; MacKay, 1992), and lesion experiments have

demonstrated that reaching to stationary stimuli is disrupted after the removal of area 7a (LaMotte and Acuna, 1978; Rushworth *et al.*, 1997). In this sense, the neurons in area 7a that responded exclusively during the interception task and showed significant effects on hand force in the multiple regression analysis, may well be part of the initial command signal to intercept moving stimuli using visual information (Mountcastle *et al.*, 1975).

There are several possible anatomical routes by which information from area 7a could reach the motor cortex. The first is through the weak but direct connections to dorsal premotor cortex (Tanne-Gariepy *et al.*, 2002). A second cortico-cortical pathway is via area 7m which projects to dorsal premotor cortex (Cavada and Goldman-Rakic, 1989a; Johnson *et al.*, 1996), or via area 7b which projects to area 5 (Cavada and Goldman-Rakic, 1989a). In turn, dorsal premotor cortex and area 5 are reciprocally linked to motor cortex (Muakkassa and Strick, 1979; Caminiti *et al.*, 1985; Tokuno and Tanji, 1993). Another possible route could be through dorsal prefrontal cortex (Cavada and Goldman-Rakic, 1989b) which is connected to the dorsal premotor cortex (Goldman-Rakic, 1987; Lu *et al.*, 1994). Finally, area 7a may influence many premotor areas and the motor cortex through its extensive subcortical connections to the basal ganglia and the pontocerebellar systems (May and Andersen, 1986; Yeterian and Pandya, 1993) that reach the precentral areas through the 'motor' thalamus, including the ventrolateral and ventral anterior nuclei (Percheron *et al.*, 1996; Hoover and Strick, 1999).

Visual motion information can reach the motor cortex through several pathways, as mentioned above. At the neurophysiological level, responses to visually moving stimuli have been reported previously (Wannier *et al.*, 1989; Port *et al.*, 2001), including complex stimuli such as optic flow (Merchant *et al.*, 2001b). In addition, it has been observed that the activity of motor cortical cells is modulated by the initial stimulus velocity during an interception task (Lee *et al.*, 2001). Therefore, motor cortical cells have access to specific aspects of visual motion information, even in the absence of a motor response. However, there is still the possibility that the NOGO activity is not related to the visual stimulus, but to the preparation of an inhibited movement, that is planned but not executed. We think that this is unlikely, since not only the descriptive but also the quantitative analysis of the motor cortical activity revealed a strong visual motion signal during the interception and NOGO tasks. In addition, the EMG analysis showed that the temporal profile of muscular activation during the interception task was directly linked to the onset of the hand force pulse, not to the stimulus parameters.

In conclusion, area 7a and motor cortex are probably part of a parieto-frontal system engaged in the interception of moving targets. Under this framework, neurons in area 7a process the high level features of the circularly moving stimuli and produce an early command signal for stimulus interception. This information can be transmitted through different potential nodes of this distributed system to the motor cortex, where some aspects of the visual stimulus are still processed to trigger the interception movement using a predictive mechanism.

## Notes

This work was supported by United States Public Health Service grant PSMH48185, the United States Department of Veterans Affairs, and the American Legion Brain Sciences Chair.

Address correspondence to: Dr Apostolos P. Georgopoulos, Brain Sciences Center (11B), VAMC, One Veterans Drive, Minneapolis, MN 55417, USA. Email: omega@umn.edu.

## References

- Albright TD (1984) Direction and orientation selectivity of neurons in visual area MT of the macaque. *J Neurophysiol* 52:1106-1130.
- Andersen RA (1997) Neural mechanisms of visual motion perception in primates. *Neuron* 18:865-872.
- Andersen RA, Buneo CA (2002) Intentional maps in posterior parietal cortex. *Annu Rev Neurosci* 25:189-220.
- Andersen RA, Snowden RJ, Treue S, Graziano M (1990) Hierarchical processing of motion in the visual cortex of monkey. *Cold Spring Harb Symp Quant Biol* 55:741-748.
- Ashe J (1997) Force and the motor cortex. *Behav Brain Res* 87:255-269.
- Ashe J, Georgopoulos AP (1994) Movement parameters and neural activity in motor cortex and area 5. *Cereb Cortex* 4:590-600.
- Barash S, Bracewell RM, Fogassi L, Gnadt JW, Andersen RA (1991) Saccade-related activity in the lateral intraparietal area. I. Temporal properties; comparison with area 7a. *J Neurophysiol* 66:1095-1108.
- Battaglia-Mayer A, Ferraina S, Genovesio A, Marconi B, Squatrito S, Molinari M, Lacquaniti F, Caminiti R (2001) Eye-hand coordination during reaching. II. An analysis of the relationships between visuomanual signals in parietal cortex and parieto-frontal association projections. *Cereb Cortex* 11:528-544.
- Caminiti R, Zeger S, Johnson PB, Urbano A, Georgopoulos AP (1985) Corticocortical efferent systems in the monkey: a quantitative spatial analysis of the tangential distribution of cells of origin. *J Comp Neurol* 241:405-419.
- Caminiti R, Ferraina S, Mayer AB (1998) Visuomotor transformations: early cortical mechanisms of reaching. *Curr Opin Neurobiol* 8:753-761.
- Cavada C, Goldman-Rakic PS (1989a) Posterior parietal cortex in the rhesus monkey. I. Parcellation of areas based on distinctive limbic and sensory corticocortical connections. *J Comp Neurol* 287:393-421.
- Cavada C, Goldman-Rakic PS (1989b) Posterior parietal cortex in the rhesus monkey. II. Evidence for segregated corticocortical networks linking sensory and limbic areas with the frontal lobe. *J Comp Neurol* 287:422-445.
- Colby CL, Goldberg ME (1999) Space and attention in parietal cortex. *Annu Rev Neurosci* 22:319-349.
- Collewijn H (1972) Latency and gain of the rabbit's optokinetic reactions to small movements. *Brain Res* 36:59-70.
- Cox DR, Lewis PA (1966) The statistical analysis of series of events. London: Chapman & Hall.
- Draper NR, Smith H (1981) Applied regression analysis. New York: John Wiley & Sons.
- Evarts EV (1981) Handbook of physiology. The nervous system II. Bethesda, MD: American Physiological Society.
- Felleman DJ, Van Essen DC (1991) Distributed hierarchical processing in the primate cerebral cortex. *Cereb Cortex* 1:1-47.
- Georgopoulos AP (1999) News in motor cortical physiology. *New Physiol Sci* 14:64-68.
- Georgopoulos AP, Ashe J, Smyrnis N, Taira M (1992) Motor cortex and the coding of force. *Science* 256:1692-1695.
- Goldman-Rakic PS (1987) Motor control function of the prefrontal cortex. *CIBA Found Symp* 132:187-200.
- Hatsopoulos N, Gabbiani F, Laurent G (1995) Elementary computation of object approach by a wide-field visual neuron. *Science* 270:1000-1003.
- Hoover JE, Strick PL (1999) The organization of cerebellar and basal ganglia outputs to primary motor cortex as revealed by retrograde transneuronal transport of herpes simplex virus type 1. *J Neurosci* 19:1446-1463.
- Humphrey DR, Schmidt EM, Thompson WD (1970) Predicting measures of motor performance from multiple cortical spike trains. *Science* 170:758-762.

- Johnson PB, Ferraina S, Bianchi L, Caminiti R (1996) Cortical networks for visual reaching: physiological and anatomical organization of frontal and parietal lobe arm regions. *Cereb Cortex* 6:102-119.
- LaMotte, RH and Acuna, C (1978) Defects in accuracy of reaching after removal of posterior parietal cortex in monkeys. *Brain Res* 139:309-326.
- Lee DN (1976) A theory of visual control of braking based on information about time-to-collision. *Perception* 5:437-459.
- Lee D, Port NL, Georgopoulos AP (1997) Manual interception of moving targets. II. On-line control of overlapping submovements. *Exp Brain Res* 116:421-433.
- Lee D, Port NL, Kruse W, Georgopoulos AP (2001) Neuronal clusters in the primate motor cortex during interception of moving targets. *J Cogn Neurosci* 13:319-331.
- Lu MT, Preston JB, Strick PL (1994) Interconnections between the prefrontal cortex and the premotor areas in the frontal lobe. *J Comp Neurol* 341:375-392.
- MacKay WA (1992) Properties of reach-related neuronal activity in cortical area 7A. *J Neurophysiol* 67:1335-1345.
- Marconi B, Genovesio A, Battaglia-Mayer A, Ferraina S, Squatrito S, Molinari M, Lacquaniti F, Caminiti R (2001) Eye-hand coordination during reaching. I. Anatomical relationships between parietal and frontal cortex. *Cereb Cortex* 11:513-527.
- Mardia KV (1972) Statistics of directional data. New York: Academic Press.
- Maunsell JH, Van Essen DC (1983a) Functional properties in middle temporal visual area of the macaque monkey. I. Selectivity for stimulus direction, speed, and orientation. *J Neurophysiol* 49:1129-1147.
- Maunsell JH, Van Essen DC (1983b) The connections of the middle temporal visual area (MT) and their relationship to a cortical hierarchy in the macaque monkey. *J Neurosci* 3:2563-2586.
- May JG, Andersen RA (1986) Different patterns of corticopontine projections from separate cortical fields within the inferior parietal lobule and the dorsal prelunate gyrus of the macaque. *Exp Brain Res* 63:265-278.
- Merchant H, Battaglia-Mayer A, Georgopoulos AP (2001a) Responses of motor cortical cells during interception of circularly moving targets. *Soc Neurosci Abstr* 27:322.
- Merchant H, Battaglia-Mayer A, Georgopoulos AP (2001b) Effects of optic flow in motor cortex and area 7a. *J Neurophysiol* 87:1937-1954.
- Merchant H, Battaglia-Mayer A, Georgopoulos AP (2003a) Interception of real and apparent motion targets: psychophysics in humans and monkeys. *Exp Brain Res* (in press).
- Merchant H, Battaglia-Mayer A, Georgopoulos AP (2003b) Neural responses to real and apparent motion stimuli in motor cortex and area 7a. Submitted for publication.
- Merchant H, Battaglia-Mayer A, Georgopoulos AP (2003c) Functional organization of parietal neuronal responses to optic flow stimuli. *J Neurophysiol* (in press).
- Motter BC, Mountcastle VB (1981) The functional properties of the light-sensitive neurons of the posterior parietal cortex studied in waking monkeys: foveal sparing and opponent vector organization. *J Neurosci* 1:3-26.
- Mountcastle VB (1978) An organizing principle for cerebral function. In: *The mindful brain* (Edelman GM, Mountcastle VB, eds), pp. 7-50. Cambridge, MA: MIT Press.
- Mountcastle VB, Lynch JC, Georgopoulos A, Sakata H, Acuna C (1975) Posterior parietal association cortex of the monkey: command functions for operations within extrapersonal space. *J Neurophysiol* 38:871-908.
- Muakkassa KF, Strick PL (1979) Frontal lobe inputs to primate motor cortex: evidence for four somatotopically organized 'premotor' areas. *Brain Res* 177:176-182.
- Percheron G, Francois C, Talbi B, Yelnik J, Fenelon G (1996) The primate motor thalamus. *Brain Res Rev* 22:93-181.
- Port NL, Pellizzer G, Georgopoulos AP (1996) Intercepting real and path-guided apparent motion targets. *Exp Brain Res* 110:298-307.
- Port NL, Lee D, Dassonville P, Georgopoulos AP (1997) Manual interception of moving targets. I. Performance and movement initiation. *Exp Brain Res* 116:406-420.
- Port NL, Kruse W, Lee D, Georgopoulos AP (2001) Motor cortical activity during interception of moving targets. *J Cogn Neurosci* 13:306-318.
- Richmond BJ, Optican LM (1987) Temporal encoding of two-dimensional patterns by single units in primate inferior temporal cortex. II. Quantification of response waveform. *J Neurophysiol* 57:147-161.
- Rind CF, Simmons PJ (1999) Seeing what is coming: building collision-sensitive neurons. *Trends Neurosci* 22:215-220.
- Rizzolatti G, Luppino G (2001) The cortical motor system. *Neuron* 31:889-901.
- Rushworth MF, Nixon PD, Passingham RE (1997) Parietal cortex and movement. I. Movement selection and reaching. *Exp Brain Res* 117:292-310.
- Sakata H, Shibutani H, Ito Y, Tsurugai K (1986) Parietal cortical neurons responding to rotary movement of visual stimulus in space. *Exp Brain Res* 61:658-663.
- Sakata H, Shibutani H, Ito Y, Tsurugai K, Mine S, Kusunoki, M (1994) Functional properties of rotation-sensitive neurons in the posterior parietal association cortex of the monkey. *Exp Brain Res* 101:183-202.
- Sakata H, Taira M, Kusunoki M, Murata A, Tanaka Y, Tsutsui K (1998) Neural coding of 3D features of objects for hand action in the parietal cortex of the monkey. *Philos Trans R Soc Lond B Biol Sci* 353:1363-1373.
- Schwartz AB, Kettner RE, Georgopoulos AP (1988) Primate motor cortex and free arm movements to visual targets in three-dimensional space. I. Relations between single cell discharge and direction of movement. *J Neurosci* 8:2913-2927.
- Schwartz AB (1993) Motor cortical activity during drawing movements: population representation during sinusoid tracing. *J Neurophysiol* 70:28-36.
- Siegel RM, Read HL (1997) Analysis of optic flow in the monkey parietal area 7a. *Cereb Cortex* 7:327-346.
- Snedecor GW, Cochran WG (1989) Statistical methods. Ames, IA: Iowa State University Press.
- Taira M, Boline J, Smyrnis N, Georgopoulos AP, Ashe J (1996) On the relations between single cell activity in the motor cortex and the direction and magnitude of three-dimensional static isometric force. *Exp Brain Res* 109:367-376.
- Tanne-Gariepy J, Rouiller EM, Boussaoud D (2002) Parietal inputs to dorsal versus ventral premotor areas in the macaque monkey: evidence for largely segregated visuomotor pathways. *Exp Brain Res* 145:91-103.
- Thach WT (1978) Correlation of neural discharge with pattern and force of muscular activity, joint position, and direction of intended next movement in motor cortex and cerebellum. *J Neurophysiol* 41:654-676.
- Tokuno H, Tanji J (1993) Input organization of distal and proximal forelimb areas in the monkey primary motor cortex: a retrograde double labeling study. *J Comp Neurol* 333:199-209.
- van Donkelaar P, Lee RG, Gellman RS (1992) Control strategies in directing the hand to moving targets. *Exp Brain Res* 91:151-161.
- Wannier TM, Maier MA, Hepp-Reymond MC (1989) Responses of motor cortex neurons to visual stimulation in the alert monkey. *Neurosci Lett* 98:63-68.
- Yeterian EH, Pandya DN (1993) Striatal connections of the parietal association cortices in rhesus monkeys. *J Comp Neurol* 332:175-197.